# THE NARROW CAPTURE PROBLEM WITH PARTIALLY ABSORBING TARGETS AND STOCHASTIC RESETTING*

PAUL C. BRESSLOFF† AND RYAN D. SCHUMM†

**Abstract.** We consider a particle undergoing diffusion with stochastic resetting in a bounded domain $\mathcal{U} \subset \mathbb{R}^d$ for $d = 2, 3$. The domain is perforated by a set of partially absorbing spherical targets within which the particle may be absorbed at a rate $\kappa$. Each target is assumed to be much smaller than $|\mathcal{U}|$, which allows us to use asymptotic and Green's function methods to solve the diffusion equation in Laplace space. In particular, we construct an inner solution within the interior and local exterior of each target and match it with an outer solution in the bulk of $\mathcal{U}$. This yields an asymptotic expansion of the Laplace transformed flux into each target in powers of $\nu = -1/\ln \epsilon$ ($d = 2$) and $\epsilon$ ($d = 3$), respectively, where $\epsilon$ is the nondimensionalized target size. The fluxes determine how the mean first passage time (MFPT) to absorption depends on the reaction rate $\kappa$ and the resetting rate $r$. For a range of parameter values, the MFPT is a unimodal function of $r$, with a minimum at an optimal resetting rate $r_{\text{opt}}$ that depends on $\kappa$ and the target configuration.

**1. Introduction.** Chemical reaction kinetics depend on the transport mechanisms that enable two reactants A and B to meet within their reaction radius [35]. The transport process can be formulated as a searcher A looking for a target B, and the effective reaction rate is related to a first passage time (FPT) problem [26]. Within the interior of living cells, molecular concentrations tend to be dilute so that there are very few copies of reactants. This means that the corresponding search process involves finding a small hidden target within a much larger bounded domain—the so-called narrow capture problem. The small size of the targets can be exploited to solve the FPT problem using matched asymptotic expansions and Green's function methods [37, 4, 14, 13, 12, 15, 27, 28, 30, 25]. Given the fact that passive diffusion results in unrealistically slow reaction rates, there has been considerable interest in identifying both natural and artificial mechanisms for speeding up the underlying search process. One major example is random intermittent transport, in which a reactant switches between passive diffusion and active ballistic motion [31, 1]; the latter could be mediated by molecular motors transiently binding diffusing reactant molecules within the cellular environment. One finds that intermittent transport can significantly enhance chemical reactivity and often leads to a nontrivial optimization of reaction rates. (The general theory of random intermittent search processes is reviewed in [2].) An idealized version of a random intermittent search process is diffusion with stochastic resetting or restart, whereby the position of a Brownian particle is reset to a fixed location at a random sequence of times, which is typically (but not necessarily) generated by a Poisson process [16, 17, 18]. Moreover, there typically

---

†Department of Mathematics, University of Utah, Salt Lake City, UT 84112 USA (bressloff@math.utah.edu, schumm@math.utah.edu).
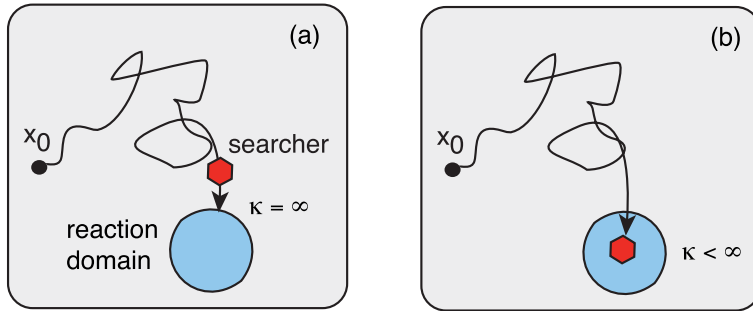
FIG. 1.1. *Two models of a chemical reaction.* (a) *A diffusing particle reacts as soon as it reaches the boundary $\partial\Omega$ of the reaction domain $\Omega$. The surface $\partial\Omega$ acts as a perfect absorber. Alternatively, the surface may acts as a partial absorber with a finite reaction rate $\kappa$. (b) A particle can diffuse in and out of the reaction domain and reacts at a finite rate $\kappa$ within the domain. In the presence of stochastic resetting (not shown), the particle can instantaneously return to its initial point $\mathbf{x}_0$ at a rate $r$ prior to reacting, after which the search process is restarted.*

exists an optimal resetting rate for minimizing the mean first passage time (MFPT) to find a target. The simplicity of the resetting protocol means that it can be applied to a wide range of stochastic processes beyond Brownian motion; see the recent review [20] and references therein.

There are a few different reaction scenarios that can be combined with the transport process, as illustrated in Figure 1.1. In the case of a diffusion-limited reaction, as soon as the particle hits the boundary $\partial\Omega$ of the reaction domain or target $\Omega$ it reacts instantaneously (totally absorbing target boundary); see Figure 1.1(a). This can be implemented by imposing the Dirichlet boundary condition $p(\mathbf{x}, t) = 0$ for all $\mathbf{x} \in \partial\Omega$, where $p(\mathbf{x}, t)$ is the probability density for the position of a diffusing particle. Alternatively, there could be a nonzero probability that the particle is reflected rather than absorbed (partially absorbing target boundary). This is typically modeled using a Robin boundary condition, namely, $D\nabla p(\mathbf{x}, t) \cdot \mathbf{n} + \kappa_0 p(\mathbf{x}, t) = 0$ for all $\mathbf{x} \in \partial\Omega$. Here $D$ is the diffusivity and $\kappa$ is a reactivity constant. The partially absorbing example suggests a second type of target interaction, as shown in Figure 1.1(b). Now a particle can diffuse in and out of the reaction domain $\Omega$ and reacts at a finite rate $\kappa$ when inside the domain. The target thus acts like a partially absorbing chemical substrate. One important example is the passive or active intracellular transport of a vesicle (particle) along the axon or dendrite of a neuron, where absorption represents the transfer of the vesicle to a synaptic target within the surface membrane of the neuron [5, 7]. (It is also possible to develop a more general probabilistic formulation of diffusion-mediated surface reactions using the encounter-based approach developed by Grebenkov [23, 24], which has recently been extended to partially absorbing interior targets [10].)

We have previously analyzed the effects of stochastic resetting on diffusion in $\mathbb{R}^d$ in the case of a single spherical target with a partially absorbing interior [36]. This type of boundary value problem can be solved exactly by exploiting spherical symmetry. However, in the case of diffusion in a bounded domain with multiple targets, it is not usually possible to obtain an exact solution so that some form of approximation scheme is necessary. This motivates the study of narrow capture problems, at least when the targets are small compared to the size of the bulk domain. Previous studies of the narrow capture problem have focused primarily on partially

or totally absorbing target boundaries without stochastic resetting. However, we have recently shown how asymptotic methods can be extended to incorporate the effects of stochastic resetting by solving the diffusion equation in Laplace space and determining the resulting flux into each target [8, 9]; the Laplace transformed flux acts as a generator of statistical quantities such as the MFPT to absorption. In this paper, we analyze the two-dimensional (2D) and three-dimensional (3D) narrow capture problem with stochastic resetting and partially absorbing targets, as opposed to partially reflecting target boundaries. We proceed by considering the diffusion equation in a bounded, perforated domain $\mathcal{U} \subset \mathbb{R}^d$, $d = 2, 3$. Working in Laplace space, we construct an inner solution that holds within the interior and local exterior of each reaction domain, and then we match it with an outer solution in the bulk $\mathcal{U}$. This yields an asymptotic expansion of the Laplace transformed flux into each reaction domain in powers of $\nu = -1/\ln \epsilon$ $(d = 2)$ and $\epsilon$ $(d = 3)$, where $\epsilon$ is the nondimensionalized target size. The Laplace transformed fluxes are used to determine how the MFPT to absorption depends on the reaction rate $\kappa$ and the resetting rate $r$. For a range of parameter values, we find that the MFPT is a unimodal function of $r$, with a minimum at an optimal resetting rate $r_{\text{opt}}$ that depends on $\kappa$ and the target configuration. The narrow escape problem is formulated in section 2 , the matched asymptotic expansions for $d = 2$ and $d = 3$ are carried out in section 3 and section 4, respectively, and comparisons of the theoretical results with numerical simulations are presented in section 5.

**2. The narrow capture problem.** Consider a set of partial absorbing targets $\mathcal{U}_k \subset \mathcal{U}$, $k = 1, \ldots, N$, in a bounded search domain $\mathcal{U} \subset \mathbb{R}^d$, and set $\bigcup_{k=1}^{N} \mathcal{U}_k = \mathcal{U}_a$; see Figure 2.1. Whenever the particle is within $\mathcal{U}_k$ it can be absorbed (react) at a rate $\kappa$. Each target is taken to be much smaller than $\mathcal{U}$, that is, $|\mathcal{U}_j| \sim \epsilon^d |\mathcal{U}|$ with $\mathcal{U}_j \to \mathbf{x}_j \in \mathcal{U}$ uniformly as $\epsilon \to 0$, $j = 1, \ldots, N$. In addition, the targets are assumed to be well separated with $|\mathbf{x}_i - \mathbf{x}_j| = O(1)$, $j \neq i$, and $\text{dist}(x_j, \partial\mathcal{U}) = O(1)$ for all $i = 1, \ldots, N$. In order to develop the analysis we will assume, for simplicity, that each target is a $d$-dimensional sphere of radius $\epsilon \ell_j$: $\mathcal{U}_i = \{\mathbf{x} \in \mathcal{U}, \ |\mathbf{x} - \mathbf{x}_i| \leq \epsilon \ell_i\}$.

**2.1. Diffusion without resetting.** Let $p(\mathbf{x}, t | \mathbf{x}_0)$ be the probability density that at time $t$ a particle is at $\mathbf{X}(t) = \mathbf{x}$, having started at position $\mathbf{x}_0$. We will set $p = q$ for all $\mathbf{x} \in \mathcal{U} \backslash \mathcal{U}_a$ and $p = p_k$ for all $\mathbf{x} \in \mathcal{U}_k$ such that
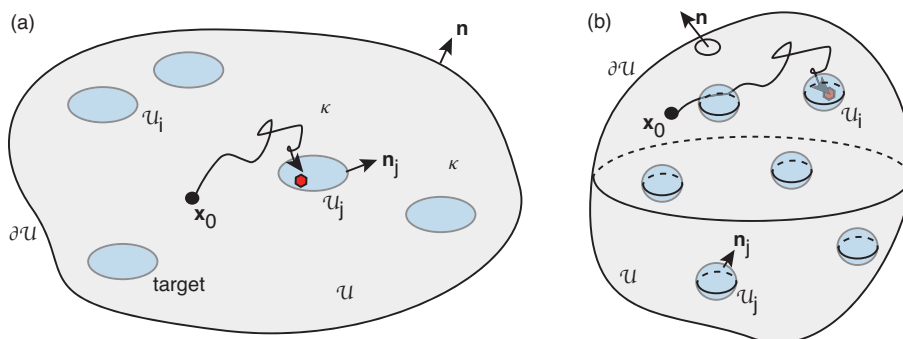


FIG. 2.1. *Random search in a domain* $\mathcal{U} \subseteq \mathbb{R}^d$ *with* $N$ *partially absorbing targets* $\mathcal{U}_j$, $j = 1, \ldots, N$. *Whenever the searcher is within the target domain* $\mathcal{U}_j$, *it can be absorbed at a rate* $\kappa$. (a) $d = 2$, (b) $d = 3$.

$$(2.1a) \qquad \frac{\partial q(\mathbf{x}, t|\mathbf{x}_0)}{\partial t} = D\nabla^2 q(\mathbf{x}, t|\mathbf{x}_0), \ \mathbf{x} \in \mathcal{U}\backslash\mathcal{U}_a,$$

$$(2.1b) \qquad \frac{\partial p_k(\mathbf{x}, t|\mathbf{x}_0)}{\partial t} = D\nabla^2 p_k(\mathbf{x}, t|\mathbf{x}_0) - \kappa p_k(\mathbf{x}, t|\mathbf{x}_0), \ \mathbf{x} \in \mathcal{U}_k,$$

together with continuity conditions at each target boundary,

$$(2.2) \qquad q(\mathbf{x}, t|\mathbf{x}_0) = p_k(\mathbf{x}, t|\mathbf{x}_0), \ \nabla q(\mathbf{x}, t|\mathbf{x}_0) \cdot \mathbf{n}_k = \nabla p_k(\mathbf{x}, t|\mathbf{x}_0) \cdot \mathbf{n}_k$$

for all $\mathbf{x} \in \partial\mathcal{U}_k$, and the exterior boundary condition

$$(2.3) \qquad \nabla q \cdot \mathbf{n} = 0, \ \mathbf{x} \in \partial\mathcal{U}.$$

Here $\kappa$ is the rate at which the particle is absorbed by a target, $\mathbf{n}$ is the outward unit normal at a point on $\partial\mathcal{U}$, and $\mathbf{n}_k$ is the outward unit normal at a point on $\mathcal{U}_k$. We will assume that the particle starts outside all of the targets, so that

$$(2.4) \qquad q(\mathbf{x}, 0|\mathbf{x}_0) = \delta(\mathbf{x} - \mathbf{x}_0), \quad p_k(\mathbf{x}, 0|\mathbf{x}_0) = 0.$$

It follows that in the limit $\kappa \to \infty$, the particle is immediately absorbed when it hits any target boundary $\partial\mathcal{U}_i$. The latter then acts as a perfect absorber.

The probability flux into the $k$th target at time $t$ is

$$(2.5) \qquad J_k(\mathbf{x}_0, t) = \kappa \int_{\mathcal{U}_k} p_k(\mathbf{x}, t|\mathbf{x}_0)d\mathbf{x}, \ k = 1, \dots, N.$$

Hence, the splitting probability that the particle is eventually captured by the $k$th target is

$$(2.6) \qquad \pi_k(\mathbf{x}_0) = \int_0^\infty J_k(\mathbf{x}_0, t')dt' = \widetilde{J}_k(\mathbf{x}_0, 0),$$

where $\widetilde{J}_k(\mathbf{x}_0, s)$ denotes the Laplace transform of $J_k(\mathbf{x}_0, t)$. Let $Q(\mathbf{x}_0, t)$ denote the survival probability that the particle hasn't been absorbed by a target in the time interval $[0, t]$, having started at $\mathbf{x}_0$:

$$(2.7) \qquad Q(\mathbf{x}_0, t) = \int_{\mathcal{U}} p(\mathbf{x}, t|\mathbf{x}_0)d\mathbf{x} = \int_{\mathcal{U}\backslash\mathcal{U}_a} q(\mathbf{x}, t|\mathbf{x}_0)d\mathbf{x} + \sum_{k=1}^N \int_{\mathcal{U}_k} p_k(\mathbf{x}, t|\mathbf{x}_0)d\mathbf{x}.$$

Differentiating both sides of this equation with respect to $t$ and using equations (2.1)a,b implies that

$$\frac{\partial Q(\mathbf{x}_0, t)}{\partial t} = D \int_{\mathcal{U}\backslash\mathcal{U}_a} \nabla^2 q(\mathbf{x}, t|\mathbf{x}_0)d\mathbf{x} + \sum_{k=1}^N \int_{\mathcal{U}_k} \left[ D\nabla^2 p_k(\mathbf{x}, t|\mathbf{x}_0) - \kappa p_k(\mathbf{x}, t|\mathbf{x}_0) \right] d\mathbf{x}$$

$$= -\sum_{k=1}^N \int_{\partial\mathcal{U}_k} \nabla q \cdot \mathbf{n}_k d\sigma + \sum_{k=1}^N \int_{\partial\mathcal{U}_k} \nabla p_k \cdot \mathbf{n}_k d\sigma - \kappa \sum_{k=1}^N \int_{\mathcal{U}_k} p_k(\mathbf{x}, t|\mathbf{x}_0)d\mathbf{x}$$

$$(2.8) \qquad = -\sum_{k=1}^N J_k(\mathbf{x}_0, t),$$

where we have used the current conservation condition in (2.2). Laplace transforming (2.8) and imposing the initial condition $Q(\mathbf{x}_0, 0) = 1$ gives

$$(2.9) \qquad s\widetilde{Q}(\mathbf{x}_0, s) - 1 = -\sum_{k=1}^{N} \widetilde{J}_k(\mathbf{x}_0, s).$$

In the case of a bounded domain $\mathcal{U}$, the particle is eventually absorbed by one of the targets with probability one, which means that $\lim_{t\to\infty} Q(\mathbf{x}_0, t) = \lim_{s\to 0} s\widetilde{Q}(\mathbf{x}_0, s) = 0$. Hence, $\sum_{k=1}^{N} \widetilde{J}_k(\mathbf{x}_0, s) = \sum_{k=1}^{N} \pi_k(\mathbf{x}_0) = 1$. The normalized flux $J_k(\mathbf{x}_0, t)/\pi_k(\mathbf{x}_0)$ is the conditional FPT density for absorption by the $k$th target. Hence, the $k$th conditional MFPT is

$$(2.10) \qquad T_k(\mathbf{x}_0) = \frac{1}{\pi_k(\mathbf{x}_0)} \int_0^\infty t J_k(\mathbf{x}_0, t) dt = -\frac{1}{\pi_k(\mathbf{x}_0)} \left. \frac{\partial}{\partial s} \widetilde{J}_k(\mathbf{x}_0, s) \right|_{s=0}.$$

The corresponding unconditional MFPT is

$$(2.11) \qquad T(\mathbf{x}_0) \equiv \sum_{k=1}^{N} \pi_k(\mathbf{x}_0) T_k(\mathbf{x}_0) = -\frac{\partial}{\partial s} \sum_{k=1}^{N} \widetilde{J}_k(\mathbf{x}_0, s) \bigg|_{s=0} = \widetilde{Q}(\mathbf{x}_0, 0).$$

Note that if the domain $\mathcal{U}$ were unbounded, then $T(\mathbf{x}_0)$ would be infinite.

**2.2. Diffusion with resetting.** Now suppose that prior to being absorbed by one of the targets, the particle can instantaneously reset to a fixed location $\mathbf{x}_r$ at a random sequence of times generated by an exponential probability density $\psi(\tau) = re^{-r\tau}$, where $r$ is the resetting rate. The probability that no resetting has occurred up to time $\tau$ is then $\Psi(\tau) = 1 - \int_0^\tau \psi(s)ds = e^{-r\tau}$. In the following we identify $\mathbf{x}_r$ with the initial position by setting $\mathbf{x}_0 = \mathbf{x}_r$.[1] Equations (2.1)a,b become

$$(2.12a)$$
$$\frac{\partial q_r(\mathbf{x}, t|\mathbf{x}_0)}{\partial t} = D\nabla^2 q_r(\mathbf{x}, t|\mathbf{x}_0) - r q_r(\mathbf{x}, t|\mathbf{x}_0) + r Q_r(\mathbf{x}_0, t)\delta(\mathbf{x} - \mathbf{x}_0), \ \mathbf{x} \in \mathcal{U}\backslash\mathcal{U}_a,$$
$$(2.12b)$$
$$\frac{\partial p_{r,k}(\mathbf{x}, t|\mathbf{x}_0)}{\partial t} = D\nabla^2 p_{r,k}(\mathbf{x}, t|\mathbf{x}_0) - (\kappa + r)p_{r,k}(\mathbf{x}, t|\mathbf{x}_0), \ \mathbf{x} \in \mathcal{U}_k.$$

Here $q_r$ and $p_{r,k}$ are the resetting analogues of $q$ and $p_k$, respectively, whereas $Q_r(\mathbf{x}_0, t)$ denotes the survival probability in the presence of resetting:

$$(2.13) \quad Q_r(\mathbf{x}_0, t) = \int_\mathcal{U} p_r(\mathbf{x}, t|\mathbf{x}_0)d\mathbf{x} = \int_{\mathcal{U}\backslash\mathcal{U}_a} q_r(\mathbf{x}, t|\mathbf{x}_0)d\mathbf{x} + \sum_{k=1}^{N} \int_{\mathcal{U}_k} p_{r,k}(\mathbf{x}, t|\mathbf{x}_0)d\mathbf{x}.$$

Equations (2.12) are supplemented by the continuity conditions

$$(2.14) \qquad q_r(\mathbf{x}, t|\mathbf{x}_0) = p_{r,k}(\mathbf{x}, t|\mathbf{x}_0), \ \nabla q_r(\mathbf{x}, t|\mathbf{x}_0) \cdot \mathbf{n}_k = \nabla p_{r,k}(\mathbf{x}, t|\mathbf{x}_0) \cdot \mathbf{n}_k$$

---

[1]For simplicity we do not include resetting delays such as finite return times and refractory periods, nor do we include nonexponential resetting statistics [11, 32, 33, 19, 3, 34, 6]. Another possible generalization would be to take the reset point $\mathbf{x}_0$ to be randomly distributed over some compact subset of $\mathcal{U}$. For example, in the case of a single spherical target in $\mathbb{R}^d$, the initial/reset point is often taken to be randomly distributed on a sphere so that one can exploit spherical symmetry to solve the associated boundary value problem [18, 36]. Choosing a distributed reset point does not change the basic results.

for all $\mathbf{x} \in \partial \mathcal{U}_k$, and the exterior boundary condition

$$(2.15) \qquad \nabla q_r \cdot \mathbf{n} = 0, \ \mathbf{x} \in \partial \mathcal{U}.$$

$Q_r$ can be related to the survival probability without resetting, which is denoted by $Q$, using a last renewal equation [16, 17, 20]; this holds irrespective of whether the target is partially or totally absorbing, since the reactivity $\kappa$ is a constant:

$$(2.16) \qquad Q_r(\mathbf{x}_0, t) = \mathrm{e}^{-rt} Q(\mathbf{x}_0, t) + r \int_0^t Q(\mathbf{x}_0, \tau) Q_r(\mathbf{x}_0, t - \tau) \mathrm{e}^{-r\tau} d\tau.$$

The first term on the right-hand side represents trajectories with no resettings. The integrand in the second term is the contribution from trajectories that last reset at time $\tau \in (0, t)$ and consists of the product of the survival probability starting from $\mathbf{x}_0$ with resetting up to time $t - \tau$ and the survival probability starting from $\mathbf{x}_0$ without any resetting for the time interval $\tau$. Laplace transforming the last renewal equation and rearranging shows that

$$(2.17) \qquad \widetilde{Q}_r(\mathbf{x}_0, s) = \frac{\widetilde{Q}(\mathbf{x}_0, r + s)}{1 - r\widetilde{Q}(\mathbf{x}_0, r + s)}.$$

It is also possible to derive (2.17) directly from the forward equations. Here we sketch the basic argument. Laplace transforming equations (2.12) gives

(2.18a)
$$D\nabla^2 \widetilde{q}_r(\mathbf{x}, s|\mathbf{x}_0) - (r + s)\widetilde{q}_r(\mathbf{x}, s|\mathbf{x}_0) = -(1 + r\widetilde{Q}_r(\mathbf{x}_0, s))\delta(\mathbf{x} - \mathbf{x}_0), \ \mathbf{x} \in \mathcal{U} \backslash \mathcal{U}_a,$$
(2.18b)
$$D\nabla^2 \widetilde{p}_{r,k}(\mathbf{x}, t|\mathbf{x}_0) - (\kappa + r + s)\widetilde{p}_{r,k}(\mathbf{x}, s|\mathbf{x}_0) = 0, \ \mathbf{x} \in \mathcal{U}_k,$$

together with the analogues of (2.2) and (2.3). Introduce the following Green's function for the modified Helmholtz equation in $\Omega \backslash \mathcal{U}_a$:

$$(2.19) \qquad D\nabla^2 G(\mathbf{x}, \alpha|\mathbf{x}_0) - (r + s)G(\mathbf{x}, \alpha|\mathbf{x}_0) = -\delta(\mathbf{x} - \mathbf{x}_0), \ \mathbf{x} \in \mathcal{U} \backslash \mathcal{U}_a,$$

$$(2.20) \qquad G(\mathbf{x}, \alpha|\mathbf{x}_0) = 0, \ \mathbf{x} \in \partial \mathcal{U}_a, \quad \nabla G(\mathbf{x}, \alpha|\mathbf{x}_0) \cdot \mathbf{n} = 0, \ \mathbf{x} \in \partial \mathcal{U},$$

with $\alpha = \sqrt{[r + s]/D}$. Using the decomposition

$$(2.21) \qquad \widetilde{q}_r(\mathbf{x}, s|\mathbf{x}_0) = u_r(\mathbf{x}, s|\mathbf{x}_0) + (1 + r\widetilde{Q}_r(\mathbf{x}_0, s))G(\mathbf{x}, \alpha|\mathbf{x}_0),$$

and imposing the Laplace transformed versions of (2.2) and (2.3), one finds

$$(2.22a) \qquad \widetilde{q}_r(\mathbf{x}, s|\mathbf{x}_0) = (1 + r\widetilde{Q}_r(\mathbf{x}_0, s))\widetilde{q}(\mathbf{x}, r + s|\mathbf{x}_0),$$
$$(2.22b) \qquad \widetilde{p}_{r,k}(\mathbf{x}, s|\mathbf{x}_0) = (1 + r\widetilde{Q}_r(\mathbf{x}_0, s))\widetilde{p}_k(\mathbf{x}, r + s|\mathbf{x}_0).$$

Substituting these expressions into the Laplace transform of (2.13) and using (2.7) implies that

$$(2.23) \qquad \widetilde{Q}_r(\mathbf{x}_0, s) = (1 + r\widetilde{Q}_r(\mathbf{x}_0, s))Q(\mathbf{x}_0, r + s),$$

which, on rearranging, yields (2.17).

Proceeding along similar lines to the derivation of (2.8), we can differentiate (2.13) with respect to $t$ and use equations (2.12) to obtain the result

$$(2.24) \qquad \frac{\partial Q_r(\mathbf{x}_0, t)}{\partial t} = -\kappa \sum_{k=1}^{N} \int_{\mathcal{U}_k} p_{r,k}(\mathbf{x}, t|\mathbf{x}_0) d\mathbf{x} \equiv -\sum_{k=1}^{N} J_{r,k}(\mathbf{x}_0, t).$$

In Laplace space we have

$$(2.25) \qquad s\widetilde{Q}_r(\mathbf{x}_0, s) - 1 = -\sum_{k=1}^{N} \widetilde{J}_{r,k}(\mathbf{x}_0, s).$$

As in the analysis of diffusion without resetting, the splitting probability is $\pi_{r,k}(\mathbf{x}_0) = \widetilde{J}_{r,k}(\mathbf{x}_0, 0)$, and the unconditional MFPT is $T_r(\mathbf{x}_0) = \widetilde{Q}_r(\mathbf{x}_0, 0)$. Using (2.17) and (2.22), these statistical quantities can then be expressed in terms of their counterparts without resetting. First, the splitting probability for absorption by the $k$th target satisfies

$$(2.26) \qquad \begin{aligned} \pi_{r,k}(\mathbf{x}_0) &= \widetilde{J}_{r,k}(\mathbf{x}_0, 0) = (1 + r\widetilde{Q}_r(\mathbf{x}_0, 0))\widetilde{J}_k(\mathbf{x}_0, r) \\ &= \left[ 1 + \frac{r\widetilde{Q}(\mathbf{x}_0, r)}{1 - r\widetilde{Q}(\mathbf{x}_0, r)} \right] \widetilde{J}_k(\mathbf{x}_0, r) = \frac{\widetilde{J}_k(\mathbf{x}_0, r)}{\sum_{j=1}^{N} \widetilde{J}_j(\mathbf{x}_0, r)}. \end{aligned}$$

Similarly, the unconditional MFPT is given by

$$(2.27) \qquad T_r(\mathbf{x}_0) = \widetilde{Q}_r(\mathbf{x}_0, 0) = \frac{\widetilde{Q}(\mathbf{x}_0, r)}{1 - r\widetilde{Q}(\mathbf{x}_0, r)} = \frac{1 - \sum_{k=1}^{N} \widetilde{J}_k(\mathbf{x}_0, r)}{r \sum_{j=1}^{N} \widetilde{J}_j(\mathbf{x}_0, r)}.$$

Equations (2.26) and (2.27) imply that the splitting probabilities and unconditional MFPT with resetting are determined by the Laplace transforms of the fluxes into the targets without resetting, $\widetilde{J}_k(\mathbf{x}_0, r)$, $k = 1, \ldots, N$. The latter depend on the absorption rate $\kappa$. In order to determine the fluxes we have to solve the Laplace transformed version of (2.1), which take the form

$$(2.28a) \qquad D\nabla^2 \widetilde{q}(\mathbf{x}, s|\mathbf{x}_0) - s\widetilde{q}(\mathbf{x}, s|\mathbf{x}_0) = -\delta(\mathbf{x} - \mathbf{x}_0), \; \mathbf{x} \in \mathcal{U}\backslash\mathcal{U}_a,$$

$$(2.28b) \qquad D\nabla^2 \widetilde{p}_k(\mathbf{x}, s|\mathbf{x}_0) - (\kappa + s)\widetilde{p}_k(\mathbf{x}, s|\mathbf{x}_0) = 0, \; \mathbf{x} \in \mathcal{U}_k,$$

together with the boundary condition $\nabla\widetilde{q}\cdot\mathbf{n} = 0$, $\mathbf{x} \in \partial\mathcal{U}$ and the continuity conditions

$$(2.28c) \qquad \widetilde{q}(\mathbf{x}, s|\mathbf{x}_0) = \widetilde{p}_k(\mathbf{x}, s|\mathbf{x}_0), \; \nabla\widetilde{q}(\mathbf{x}, s|\mathbf{x}_0) \cdot \mathbf{n}_k = \nabla\widetilde{p}_k(\mathbf{x}, s|\mathbf{x}_0) \cdot \mathbf{n}_k$$

for all $\mathbf{x} \in \partial\mathcal{U}_k$. Integrating (2.28b) over the domain $\mathcal{U}_k$ implies that

$$(2.29) \qquad (s + \kappa) \int_{\mathcal{U}_k} \widetilde{p}_k(\mathbf{x}, s|\mathbf{x}_0) = D \int_{\partial\mathcal{U}_k} \nabla\widetilde{p}_k \cdot \mathbf{n}_k d\sigma = D \int_{\partial\mathcal{U}_i} \nabla\widetilde{q} \cdot \mathbf{n}_k d\sigma.$$

In the fast absorption limit $\kappa \to \infty$, the system reduces to the scalar equation

$$(2.30)$$
$$D\nabla^2 \widetilde{q}(\mathbf{x}, s|\mathbf{x}_0) - s\widetilde{q}(\mathbf{x}, s|\mathbf{x}_0) = -\delta(\mathbf{x} - \mathbf{x}_0), \; \mathbf{x} \in \mathcal{U}\backslash\mathcal{U}_a, \; \widetilde{q}(\mathbf{x}, s|\mathbf{x}_0) = 0, \; \mathbf{x} \in \partial\mathcal{U}_a.$$

Equation (2.30) takes the form of a classical narrow capture problem, which can be analyzed using matched asymptotic expansions and Green's function methods [37, 4, 14, 13, 12, 15, 27, 28, 30, 25].

In the following two sections we further extend the analysis to the case of partially absorbing targets as described by (2.28). We consider 2D diffusion in section 3 and 3D diffusion in section 4. The details of the asymptotic analyses differ due to the well-known differences in the singular nature of the associated Green's function in 2D ($\ln |\mathbf{x} - \mathbf{x}'|$) and 3D ($1/|\mathbf{x} - \mathbf{x}'|$). In particular, carrying out the matched asymptotic expansion in 2D naturally leads to terms involving the small parameter $\nu = -1/\ln \epsilon$, which is a common feature of strongly localized perturbations in 2D domains [37]. Since $\nu \to 0$ much more slowly than $\epsilon \to 0$, it is necessary to sum over the logarithmic terms nonperturbatively in order to obtain $O(1)$ accuracy with respect to an expansion in $\epsilon$.

**3. Matched asymptotic analysis in 2D.** We first consider 2D diffusion and develop the asymptotic analysis by summing over all logarithmic terms, which is accurate to leading order in $\epsilon$. The corresponding analysis for totally absorbing targets was developed in [29, 8]. The inner solution near the $j$th target is constructed by introducing the stretched local variable $\mathbf{y} = \varepsilon^{-1}(\mathbf{x} - \mathbf{x}_j)$ and setting $U(\mathbf{y}, s|\mathbf{x}_0) = \widetilde{q}(\mathbf{x}_j + \varepsilon\mathbf{y}, s|\mathbf{x}_0)$ and $V(\mathbf{y}, s|\mathbf{x}_0) = \widetilde{p}_j(\mathbf{x}_j + \varepsilon\mathbf{y}, s|\mathbf{x}_0)$. In order to maintain effective absorption in the limit $\epsilon \to 0$, we also introduce the scaling $\kappa = \kappa_1/\epsilon^2$. Then $U, V$ satisfy to $O(\epsilon)$

$$(3.1a) \qquad \nabla_{\mathbf{y}}^2 U = 0, \ |\mathbf{y}| > \ell_j, \quad \nabla_{\mathbf{y}}^2 V = \frac{\kappa_1}{D} V_0, \ |\mathbf{y}| < \ell_j,$$

$$(3.1b) \qquad U(\mathbf{y}, s|\mathbf{x}_0) = V(\mathbf{y}, s|\mathbf{x}_0), \ \nabla_{\mathbf{y}} U \cdot \mathbf{n}_j = \nabla_{\mathbf{y}} V \cdot \mathbf{n}_j, \ |\mathbf{y}| = \ell_j.$$

The solution in the original coordinates takes the form

$$(3.2a) \qquad U(\mathbf{x}, s|\mathbf{x}_0) = A_j(\nu, s) + \nu A_j(\nu, s) \left[ \Phi(\beta\ell_j) + \log |\mathbf{x} - \mathbf{x}_j|/\ell_j \right],$$

$$(3.2b) \qquad V(\mathbf{x}, s|\mathbf{x}_0) = \frac{\nu A_j(\nu, s) \Phi(\beta\ell_j)}{I_0(\beta\ell_j)} I_0 \left( \beta\epsilon^{-1}|\mathbf{x} - \mathbf{x}_j| \right),$$

where $\nu = -1/\ln \epsilon$,

$$(3.3) \qquad \Phi = \frac{I_0(\beta\ell_j)}{\beta\ell_j I_1(\beta\ell_j)}, \quad \beta = \sqrt{\kappa_1/D},$$

and $I_n(y)$ is a modified Bessel function of the first kind.

The outer solution is constructed by shrinking each target to a single point and imposing a corresponding singularity condition that is obtained by matching with the inner solution. The outer equation is given by

$$(3.4) \qquad D\nabla^2 \widetilde{q}(\mathbf{x}, s|\mathbf{x}_0) - s\widetilde{q}(\mathbf{x}, s|\mathbf{x}_0) = -\delta(\mathbf{x} - \mathbf{x}_0)$$

for $\mathbf{x} \in \mathcal{U}\backslash\{\mathbf{x}_1, \ldots, \mathbf{x}_N\}$, together with the boundary condition $\nabla\widetilde{q} \cdot \mathbf{n} = 0$, $\mathbf{x} \in \partial\mathcal{U}$. The corresponding singularity conditions are

$$(3.5) \qquad \widetilde{q} \sim A_j(\nu, s) + \nu A_j(\nu, s) \left[ \Phi(\beta\ell_j) + \log |\mathbf{x} - \mathbf{x}_j|/\ell_j \right]$$

for $\mathbf{x} \to \mathbf{x}_j$. The next step is to introduce the Green's function of the 2D modified Helmholtz equation according to

$$(3.6a) \qquad -\delta(\mathbf{x} - \mathbf{x}_0) = D\nabla^2 G(\mathbf{x}, s|\mathbf{x}_0) - sG(\mathbf{x}, s|\mathbf{x}_0), \ \mathbf{x} \in \mathcal{U},$$

$$(3.6b) \qquad 0 = \nabla G(\mathbf{x}, s|x_0) \cdot \mathbf{n}, \ \mathbf{x} \in \partial\mathcal{U}, \int_{\mathcal{U}} G(\mathbf{x}, s|x_0) d\mathbf{x} = -\frac{1}{s}.$$

Note that $G$ can be decomposed as

$$(3.7) \qquad G(\mathbf{x}, s; \mathbf{x}_0) = -\frac{\log|\mathbf{x} - \mathbf{x}_0|}{2\pi D} + R(\mathbf{x}, s; \mathbf{x}_0),$$

where $R$ is the nonsingular part of the Green's function. We then set

$$(3.8) \qquad \widetilde{q}(\mathbf{x}, s | \mathbf{x}_0) = G(\mathbf{x}, s | x_0) + \psi(\mathbf{x}, s),$$

such that

$$(3.9) \qquad D\nabla^2 \psi(\mathbf{x}, s) - s\psi(\mathbf{x}, s) = 2\pi\nu D \sum_{j=1}^{n} A_j(\nu, s)\delta(\mathbf{x} - \mathbf{x}_j)$$

for $\mathbf{x} \in \mathcal{U}$. This is supplemented by the boundary condition $\nabla\psi \cdot \mathbf{n} = 0$ on $\partial\mathcal{U}$. It follows that $\psi$ has a solution of the form

$$(3.10) \qquad \psi(\mathbf{x}, s) = -2\pi\nu D \sum_{j=1}^{n} A_j(\nu, s) G(\mathbf{x}, s | x_j).$$

We have $N$ unknown coefficients $A_j(\nu, s)$, which are obtained by solving $N$ constraints obtained by matching the inner and outer solutions:

$$(3.11) \qquad \begin{aligned} G(\mathbf{x}_j, s | \mathbf{x}_0) &= A_j(\nu, s) \left[1 + \nu\Phi(\beta\ell_j) + 2\pi\nu D R(\mathbf{x}_j, s | \mathbf{x}_j)\right] \\ &+ 2\pi\nu D \sum_{i \neq j} A_i(\nu, s) G(\mathbf{x}_i, s | \mathbf{x}_j). \end{aligned}$$

These $N$ equations can be represented by the matrix equation

$$(3.12) \qquad \left[(1 + \nu\Phi(\beta\ell_j))\, \mathbf{I} + 2\pi\nu D \mathbf{G}^\top\right] \mathbf{a} = \mathbf{g},$$

where $\mathbf{I}$ is the $N \times N$ identity matrix,

$$(3.13) \qquad \mathbf{a} = (A_1(\nu, s), \ldots, A_N(\nu, s))^T, \quad \mathbf{g} = (G(\mathbf{x}_1, s | \mathbf{x}_0), \ldots, G(\mathbf{x}_N, s | \mathbf{x}_0))^T,$$

and $\mathbf{G}$ is an $N \times N$ matrix given by

$$(3.14) \qquad \mathbf{G}_{jj} = R(\mathbf{x}_j, s | \mathbf{x}_j), \quad \mathbf{G}_{ij} = G(\mathbf{x}_i, s | \mathbf{x}_j),\ j \neq i.$$

Inverting (3.12) yields in component form for $j = 1, \ldots, N$

$$(3.15) \qquad A_j(\nu, s) = \sum_{i=1}^{N} \left[(1 + \nu\Phi(\beta\ell_j))\, \mathbf{I} + 2\pi\nu D \mathbf{G}^\top\right]_{ji}^{-1} G(\mathbf{x}_i, s | \mathbf{x}_0).$$

This is a nonperturbative solution that sums over all logarithmic terms along analogous lines to [37].

The coefficients $A_j$ of (3.20) determine the splitting probabilities and conditional MFPTs under resetting. Using (2.29), we can write

$$(3.16) \qquad \widetilde{J}_i(\mathbf{x}_0, s) = \frac{\kappa_1 D}{\epsilon^2 s + \kappa_1} \int_{\partial\mathcal{U}_i} \nabla\widetilde{q} \cdot \mathbf{n}\, d\sigma,$$

where $\widetilde{q}$ is the inner solution (3.1a) so that

$$\nabla_{\mathbf{x}}\widetilde{q} \cdot \mathbf{n}\big|_{\mathbf{x}\in\partial\mathcal{U}_j} = \epsilon^{-1}\, \nabla_{\mathbf{y}} U_0 \cdot \mathbf{n}\big|_{|\mathbf{y}|=\ell_j} \sim \epsilon^{-1}\ell_j^{-1}\nu A_j(\nu, s).$$

Hence, to $O(1)$ in $\epsilon$

$$(3.17) \qquad \widetilde{J}_i(\mathbf{x}_0, s) \sim 2\pi\nu D A_i(\nu, s).$$

Substituting for the flux into (2.26) and (2.27) for the hitting probability $\pi_{r,k}(\mathbf{x}_0)$ and unconditional MFPT $T_r(\mathbf{x}_0)$ with resetting gives

$$(3.18) \qquad \pi_{r,k}(\mathbf{x}_0) = \frac{A_k(\nu, r)}{\sum_{j=1}^{N} A_j(\nu, r)}, \quad T_r(\mathbf{x}_0) = \frac{1 - 2\pi\nu D \sum_{k=1}^{N} A_k(\nu, r)}{2\pi\nu D r \sum_{j=1}^{N} A_j(\nu, r)}.$$

It follows from the above analysis that all information regarding absorption within a target domain $\mathcal{U}_j$, including the effective absorption rate $\kappa_1$, is contained in the function $\Phi(\beta\ell_j)$ defined in (3.3) with $\beta = \sqrt{\kappa_1/D}$. In particular, $\Phi(\beta\ell_j)$ is an exponentially decreasing function of $\beta$ with $\Phi(\beta\ell_j) \to 0$ as $\beta \to \infty$ and $\Phi(\beta\ell_j) \to \infty$ as $\beta \to 0$. It immediately follows that the results for totally absorbing targets [8] are recovered in the fast absorption limit. On the other hand, $A_j(\nu, s) \to 0$ in the limit $\kappa_1 \to 0$. The latter means that the net flux into each target is zero since there is no absorption. Hence, the dependence of $T_r$ on $\Phi(\beta\ell_j)$ implies that $T_r(\mathbf{x}_0) \to \infty$ as $\kappa_1 \to 0$, whereas it converges to the unconditional MFPT for totally absorbing target boundaries when $\kappa_1 \to \infty$.

**3.1. Example.** In order to determine the coefficients $A_k(\nu, s)$ we need to obtain accurate numerical or analytical approximations of the Green's function for the modified Helmholtz equation and solve the matrix equation (3.12). This particular issue has been addressed by Lindsay, Spoonmore, and Tzou [29], whose results can be applied to the current problem. An important step in the evaluation of the Green's function is to decompose $G$ as the sum of the free-space Green's function and a regular boundary-dependent part:

$$(3.19) \qquad G(\mathbf{x}, s; |\mathbf{x}_0) = \frac{1}{2\pi D} K_0\left(\sqrt{s/D}|\mathbf{x} - \mathbf{x}_0|\right) + \widehat{R}(\mathbf{x}, s|\mathbf{x}_0),$$

where $K_0$ is the modified Bessel function of the second kind and $\widehat{R}$ is nonsingular at $\mathbf{x} = \mathbf{x}_0$. It can be shown that for $|\mathbf{x} - \mathbf{x}_0| = O(1)$ and large $\sqrt{s/D}$, the boundary contributions to $\widehat{R}$ are exponentially small. This allows us to write

$$G(\mathbf{x}, s; |\mathbf{x}_0) \sim \frac{1}{2\pi D} K_0\left(\sqrt{s/D}|\mathbf{x} - \mathbf{x}_0|\right), \ \mathbf{x} \neq \mathbf{x}_0,$$

$$\widehat{R}(\mathbf{x}_0, s; |\mathbf{x}_0) \sim -\frac{1}{2\pi D}\left(\ln\sqrt{s/D} - \ln 2 + \gamma_c\right),$$

where $\gamma_c \approx 0.5772$ is Euler's gamma constant. It follows that the off-diagonal terms in (3.12) are exponentially smaller than the diagonal terms. Therefore, we have to leading order

$$(3.20) \qquad A_j(\nu, s) \sim \frac{(2\pi D)^{-1} K_0\left(\sqrt{s/D}|\mathbf{x}_j - \mathbf{x}_0|\right)}{1 + \nu\Phi(\beta\ell_j) - \nu\left[\ln\sqrt{s/D} - \ln 2 + \gamma_c\right]}.$$

Hence, under the boundary-free approximation, $A_j(\nu, s)$ depends on the distances of the targets from $\mathbf{x}_0$ but is independent of the shape of the domain and the absolute locations of the targets. Numerically it has been shown that such an approximation remains valid even at intermediate values of $s$ (or equivalently at intermediate times)

provided that $\mathbf{x}_0$ and $\mathbf{x}_j$, $j = 1, \ldots, N$, are not close to the boundary and there are no bottlenecks separating the targets from $\mathbf{x}_0$. This result is reinforced in the presence of resetting. Hence, under the further approximation (3.20) and assuming $\ell_j = \ell$ for all $j$, equations (3.18) become

$$(3.21) \quad \pi_{r,j}(\mathbf{x}_0) \sim \frac{K_0\left(\sqrt{r/D}|\mathbf{x}_j - \mathbf{x}_0|\right)}{\sum_{k=1}^N K_0\left(\sqrt{r/D}|\mathbf{x}_k - \mathbf{x}_0|\right)},$$

$$(3.22)$$

$$T_r(\mathbf{x}_0) \sim \frac{1}{r} \frac{1 + \nu\Phi(\beta\ell) - \nu\left[\ln\sqrt{r/D} - \ln 2 + \gamma_c\right] - \nu\sum_{k=1}^N K_0\left(\sqrt{r/D}|\mathbf{x}_k - \mathbf{x}_0|\right)}{\nu\sum_{k=1}^N K_0\left(\sqrt{r/D}|\mathbf{x}_k - \mathbf{x}_0|\right)}.$$

Note, however, that these expressions break down in the limit $r \to 0$ (no resetting). This is consistent with the fact that there is a major difference between diffusion in bounded and unbounded domains in the absence of resetting. That is, in the latter case the MFPT is infinite.

In Figure 3.1(a) we plot $T_r$ as a function of $r$ for a single target with $|\mathbf{x}_1 - \mathbf{x}_0| \equiv \rho_1 = 0.5$. A corresponding contour plot is shown in Figure 3.1(b). It can be seen that $T_r$ has a minimum at an optimal resetting rate $r_{\text{opt}}$, which is only weakly dependent on $\kappa_1$. As expected, increasing $\kappa_1$ reduces $T_r$ as the particle has a higher probability for absorption. We also note that the MFPT is most sensitive to variations in $\kappa_1$ at small resetting rates. In all cases, $T_r \to \infty$ as $r \to \infty$, which reflects the fact that if the particle resets too often, then it never has the chance to reach even the closest target. The divergence of $T_r$ can be explored further using the asymptotic expansion

$$(3.23) \qquad K_0(z) \sim \sqrt{\frac{\pi}{2z}} e^{-z}\left[1 - \frac{1}{8z} + O(z^{-2})\right], \quad z \to \infty,$$
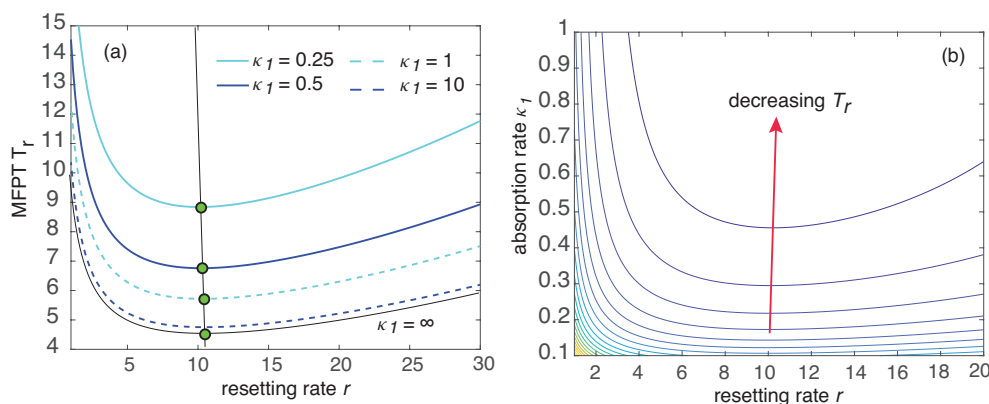


FIG. 3.1. *Single small target in $\mathbb{R}^2$ with $|\mathbf{x}_1 - \mathbf{x}_0| \equiv \rho_1 = 0.5$. (a) Plot of the MFPT $T_r(\mathbf{x}_0)$ given by (3.21) as a function of the resetting rate $r$ for various absorption rates $\kappa_1$. Other parameters are $\nu = 0.1$, $\ell = 1$, and $D = 1$. Filled circles indicate the optimal resetting rate. (b) Corresponding contour plot.*
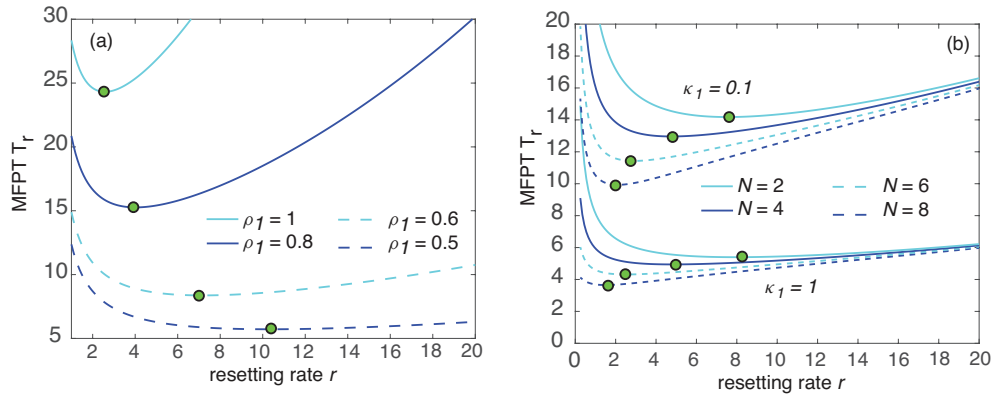
FIG. 3.2. (a) *Same as Figure* 3.1 *for different target distances* $\rho_1$ *and* $\kappa_1 = 1$. (b) $N+1$ *targets in* $\mathbb{R}^2$ *with* $|\mathbf{x}_j - \mathbf{x}_0| = \rho_0 + (j-1)\Delta\rho$ *for* $j = 1, \dots, N$. *Unconditional MFPT* $T_r(\mathbf{x}_0)$ *given by* (3.21) *as a function of the resetting rate for fixed* $\kappa_1 = 0.1, 1$. *Other parameter values are* $\nu = 0.1$, $\ell = 1$, $\rho_0 = 0.5$, $\Delta\rho = 1$, *and* $D = 1$. *Filled circles indicate the optimal resetting rate.*

which implies that

$$(3.24) \qquad T_r(\mathbf{x}) \sim (1 + \nu\Phi(\beta\ell)) \frac{\sqrt{\sqrt{r/D}|\mathbf{x}_1 - \mathbf{x}_0|}}{\nu r} \sqrt{\frac{2}{\pi}} e^{\sqrt{r/D}|\mathbf{x}_1 - \mathbf{x}_0|}$$

as $r \to \infty$. In contrast to its dependence on $\kappa_1$, the optimal resetting rate increases significantly with the target distance $\rho_1$, as shown in Figure 3.2(a). Analogous results hold for multiple target configurations as illustrated in Figure 3.2(b) for a set of $N+1$ targets whose distances from $\mathbf{x}_0$ are of the form $\rho_j = |\mathbf{x}_j - \mathbf{x}_0| = \rho_0 + (j-1)\Delta\rho$, $j = 1, \dots, N$.

**4. Matched asymptotics in 3D.** We now turn to the corresponding asymptotic analysis of the 3D problem, following along the lines of [13, 15, 9] for totally absorbing targets. The outer solution for $\widetilde{q}(\mathbf{x}, s|x_0)$ is expanded as

$$\widetilde{q}(\mathbf{x}, s|\mathbf{x}_0) \sim \widetilde{q}_0(\mathbf{x}, s|\mathbf{x}_0) + \epsilon\widetilde{q}_1(\mathbf{x}, s|\mathbf{x}_0) + \epsilon^2\widetilde{q}_2(\mathbf{x}, s|\mathbf{x}_0) + \dots.$$

The leading order term $\widetilde{q}_0$ satisfies the Laplace transformed diffusion equation without any targets within $\mathcal{U}$:

$$(4.1) \qquad D\nabla^2\widetilde{q}_0 - s\widetilde{q}_0 = -\delta(\mathbf{x} - \mathbf{x}_0), \ \mathbf{x} \in \mathcal{U}; \ \nabla\widetilde{q}_0 \cdot \mathbf{n} = 0, \ \mathbf{x} \in \partial\mathcal{U}.$$

That is, $\widetilde{q}_0 = G(\mathbf{x}, s|\mathbf{x}_0)$ where $G$ is now the Neumann Green's function of the 3D modified Helmholtz equation. The latter can be decomposed as

$$(4.2) \qquad G(\mathbf{x}, s|\mathbf{x}_0) = \frac{1}{4\pi D|\mathbf{x} - \mathbf{x}_0|} + R(\mathbf{x}, s|\mathbf{x}_0),$$

where $R$ is the regular (nonsingular) part of $G$. The higher-order contributions to the outer solution satisfy the equations

$$(4.3) \qquad D\nabla^2\widetilde{q}_n - s\widetilde{q}_n = 0, \ \mathbf{x} \in \mathcal{U}\backslash\{\mathbf{x}_1, \dots, \mathbf{x}_N\}, \ \nabla\widetilde{q}_n \cdot \mathbf{n} = 0, \ \mathbf{x} \in \partial\mathcal{U},$$

for $n \geq 1$, together with certain singularity conditions as $\mathbf{x} \to \mathbf{x}_j$, $j = 1, \dots, N$, which are determined by matching to the inner solution.

The inner solution near $\mathcal{U}_j$ is constructed in terms of the stretched local variable $\mathbf{y} = \epsilon^{-1}(\mathbf{x} - \mathbf{x}_j)$ by setting $U(\mathbf{y}, s|\mathbf{x}_0) = \widetilde{q}(\mathbf{x}_j + \varepsilon\mathbf{y}, s|\mathbf{x}_0)$ and $V(\mathbf{y}, s|\mathbf{x}_0) = \widetilde{p}_j(\mathbf{x}_j + \varepsilon\mathbf{y}, s|\mathbf{x}_0)$; see Figure 3.1. Then $U, V$ satisfy

(4.4a) $\quad D\nabla_{\mathbf{y}}^2 U - s\epsilon^2 U = 0, \quad |\mathbf{y}| > \ell_j, \quad D\nabla_{\mathbf{y}}^2 V - (s + \kappa)\epsilon^2 V = 0, \quad |\mathbf{y}| < \ell_j,$

(4.4b) $\quad U(\mathbf{y}, s|\mathbf{x}_0) = V(\mathbf{y}, s|\mathbf{x}_0), \quad \nabla_{\mathbf{y}} U \cdot \mathbf{n}_j = \nabla_{\mathbf{y}} V \cdot \mathbf{n}_j, \quad |\mathbf{y}| = \ell_j.$

Now consider a perturbation expansion of the inner solution around the $j$th target of the form

$$U \sim U_0 + \epsilon U_1 + \epsilon^2 U_2 + O(\epsilon^3), \quad V \sim V_0 + \epsilon V_1 + \epsilon^2 V_2 + O(\epsilon^3).$$

Assuming $\kappa = \kappa_1/\epsilon^2$ and $s \ll 1/\epsilon$, this yields the hierarchy of equations

(4.5a) $\quad D\nabla_{\mathbf{y}}^2 U_n(\mathbf{y}, s) = 0, \quad |\mathbf{y}| > \ell_j, \quad D\nabla_{\mathbf{y}}^2 V_n(\mathbf{y}, s) - \kappa_1 V_n = 0, \quad |\mathbf{y}| < \ell_j, \quad n = 0, 1,$

(4.5b) $\quad D\nabla_{\mathbf{y}}^2 U_n(\mathbf{y}, s) = s U_{n-2}(\mathbf{y}, s), \quad |\mathbf{y}| > \ell_j \; n \geq 2,$

(4.5c) $\quad D\nabla_{\mathbf{y}}^2 V_n - \kappa_1 V_n = s V_{n-2}, \quad |\mathbf{y}| < \ell_j, \; n \geq 2,$

(4.5d) $\quad U_n(\mathbf{y}, s) = V_n(\mathbf{y}, s), \quad \nabla_{\mathbf{y}} U_n \cdot \mathbf{n}_j = \nabla_{\mathbf{y}} V_n \cdot \mathbf{n}_j, \quad |\mathbf{y}| = \ell_j, \; n \geq 0.$

These are supplemented by far-field conditions obtained by matching $U$ with the near-field behavior of the outer solution:

(4.6) $$U_0 + \epsilon U_1 + \epsilon^2 U_2 + \cdots \sim \widetilde{q}_0 + \epsilon\widetilde{q}_1 + \epsilon^2\widetilde{q}_2 + \ldots.$$

The matching is developed iteratively along the lines of [9], starting from the known leading order contribution to the outer solution. Taylor expanding the latter near the $j$th region $\mathcal{U}_j$ yields

(4.7) $$\widetilde{q}_0 \sim G(\mathbf{x}_j, s|\mathbf{x}_0) + \nabla_{\mathbf{x}} G(\mathbf{x}, s|\mathbf{x}_0)|_{\mathbf{x}=\mathbf{x}_j}$$
$$\cdot (\mathbf{x} - \mathbf{x}_j) + \frac{1}{2}\mathbf{H}_j \cdot (\mathbf{x} - \mathbf{x}_j) \otimes (\mathbf{x} - \mathbf{x}_j) + \ldots,$$

where $\mathbf{H}_j$ is the Hessian

(4.8) $$H_j^{ab} = \left.\frac{\partial^2}{\partial x_a \partial x_b} G(\mathbf{x}, s|\mathbf{x}_0)\right|_{\mathbf{x}=\mathbf{x}_j}, \quad a, b \in \{1, 2, 3\}.$$

In terms of the stretched coordinate $\mathbf{y}$, we have

(4.9) $$\widetilde{q}_0 \sim G(\mathbf{x}_j, s|\mathbf{x}_0) + \epsilon\nabla_{\mathbf{x}} G(\mathbf{x}_j, s|\mathbf{x}_0) \cdot \mathbf{y} + \frac{\epsilon^2}{2}\mathbf{H}_j \cdot \mathbf{y} \otimes \mathbf{y} + \ldots.$$

It follows that the $n$th order derivative of $G$ will contribute to the far-field behavior of $U_n$, along with lower order derivatives of the $1, \ldots, n-1$ terms. Additional contributions will arise from the nonsingular terms in $\widetilde{q}_n$. On the other hand, the inner solution $U_n$ will have a term proportional to $1/|\mathbf{y}| = \epsilon/|\mathbf{x} - \mathbf{x}_j|$ that determines the singular behavior of $\widetilde{q}_{n+1}$ as $\mathbf{x} \to \mathbf{x}_j$. We will use this iterative matching procedure to calculate the terms $U_0, U_1, U_2$, and then use these to obtain the target fluxes to $O(\epsilon^3)$. The major difference from our previous study of the 3D narrow capture problem [9] is that we also have to match $U_n$ with the solution $V_n$ inside a target; this is crucial for quantifying how the fluxes depend on the absorption rate $\kappa_1$.

**4.1. Calculation of the leading order inner solution $U_0$.** Setting $n = 0$ in (4.5) and matching the far-field behavior of $U_0$ with the near-field behavior of $\widetilde{q}_0$ leads to the set of equations

$$(4.10a) \qquad D\nabla_{\mathbf{y}}^2 U_0(\mathbf{y}, s) = 0, \ |\mathbf{y}| > \ell_j, U_0 \sim G(\mathbf{x}_j, s|\mathbf{x}_0) \text{ as } |\mathbf{y}| \to \infty,$$

$$(4.10b) \qquad D\nabla_{\mathbf{y}}^2 V_0(\mathbf{y}, s) - \kappa_1 V_0 = 0, \quad |\mathbf{y}| < \ell_j,$$

$$(4.10c) \qquad U_0(\mathbf{y}, s) = V_0(\mathbf{y}, s), \quad \nabla_{\mathbf{y}} U_0 \cdot \mathbf{n}_j = \nabla_{\mathbf{y}} V_0 \cdot \mathbf{n}_j, \ |\mathbf{y}| = \ell_j.$$

The general solution is of the form

$$(4.11) \qquad U_0 = G(\mathbf{x}_j, s|\mathbf{x}_0) + A_0 \frac{\ell_j}{|\mathbf{y}|}, \quad V_0 = B_0 \frac{I_{1/2}(\beta|\mathbf{y}|)}{\sqrt{\beta|\mathbf{y}|}}, \quad \beta = \sqrt{\frac{\kappa_1}{D}}.$$

Note that we can write $I_{1/2}(x) = \sqrt{2/\pi} \sinh(x)/\sqrt{x}$ so that $V_0 = B_0 \sinh(\beta|\mathbf{y}|)/\beta|\mathbf{y}|$. The matching conditions then imply that

$$(4.12a) \quad G(\mathbf{x}_j, s|\mathbf{x}_0) + A_0 = \frac{B_0}{\sqrt{\beta\ell_j}} I_{1/2}(\beta\ell_j),$$

$$(4.12b)$$
$$-\frac{A_0}{\ell_j} = \frac{B_0}{\sqrt{\beta\ell_j}} \left[ \beta I'_{1/2}(\beta\ell_j) - \frac{1}{2\ell_j} I_{1/2}(\beta\ell_j) \right] = \frac{B_0}{\beta\ell_j^2} \left[ \beta\ell_j \cosh(\beta\ell_j) - \sinh(\beta\ell_j) \right].$$

Hence,

$$(4.13) \qquad U_0 = G(\mathbf{x}_j, s|\mathbf{x}_0) \left[ 1 - \Phi(\beta\ell_j) \frac{\ell_j}{|\mathbf{y}|} \right],$$

where

$$(4.14) \qquad \Phi(\beta\ell_j) = \frac{2\ell_j \beta I'_{1/2}(\beta\ell_j) - I_{1/2}(\beta\ell_j)}{2\ell_j \beta I'_{1/2}(\beta\ell_j) + I_{1/2}(\beta\ell_j)} = 1 - \frac{\tanh(\beta\ell_j)}{\beta\ell_j}.$$

It now follows that $\widetilde{q}_1$ satisfies (4.3) together with the singularity condition

$$(4.15) \qquad \widetilde{q}_1(\mathbf{x}, s) \sim -\Phi(\beta\ell_j) \frac{G_{j0}\ell_j}{|\mathbf{x} - \mathbf{x}_j|} \quad \text{as } \mathbf{x} \to \mathbf{x}_j,$$

For notational convenience, we have set $G_{j0} = G(\mathbf{x}_j, s|\mathbf{x}_0)$ and dropped the explicit dependence on $s, \mathbf{x}_0$. Hence, $\widetilde{q}_1(\mathbf{x}, s)$ satisfies the inhomogeneous equation

$$(4.16)$$

$$D\nabla^2 \widetilde{q}_1 - s\widetilde{q}_1 = 4\pi D \sum_{j=1}^{N} \Phi(\beta\ell_j) G_{j0}\ell_j \delta(\mathbf{x} - \mathbf{x}_j), \ \mathbf{x} \in \mathcal{U}, \quad \nabla\widetilde{q}_1 \cdot \mathbf{n} = 0, \ \mathbf{x} \in \partial\mathcal{U},$$

which can be solved in terms of the modified Helmholtz Green's function:

$$(4.17) \qquad \widetilde{q}_1(\mathbf{x}, s) = -4\pi D \sum_{j=1}^{N} \Phi(\beta\ell_j) G_{j0}\ell_j G(\mathbf{x}, s|\mathbf{x}_j).$$

**4.2. Calculation of higher-order terms.** The next step is to match the far-field behavior of $U_1$ with the $O(\epsilon)$ term in the expansion of $\widetilde{q}_0$; see (4.9) and the near-field behavior of $\widetilde{q}_1$ around $\mathcal{U}_j$. The latter takes the form

$$\widetilde{q}_1(\mathbf{x}, s) = -\Phi(\beta\ell_j)\left\{\frac{G_{j0}\ell_j}{|\mathbf{x} - \mathbf{x}_j|} + 4\pi D G_{j0}\ell_j R(\mathbf{x}_j, s|\mathbf{x}_j)\right\}$$
$$- 4\pi D \sum_{k \neq j}^{N} \Phi(\beta\ell_k)G_{k0}\ell_k G(\mathbf{x}_j, s|\mathbf{x}_k).$$

It follows that $U_1$ is determined by (4.5) for $n = 1$, supplemented by the condition

$$(4.18) \qquad U_1(\mathbf{y}, s) \to \nabla_{\mathbf{x}}G(\mathbf{x}_j, s|\mathbf{x}_0) \cdot \mathbf{y} - 4\pi D \sum_{k=1}^{N} \Phi(\beta\ell_k)G_{k0}\ell_k\mathcal{G}_{jk} \text{ as } |\mathbf{y}| \to \infty,$$

where $\mathcal{G}_{ij} = G(\mathbf{x}_i, s|\mathbf{x}_j)$ for $i \neq j$, and $\mathcal{G}_{ii} = R(\mathbf{x}_i, s|\mathbf{x}_i)$. It is convenient to introduce the decomposition $U_1 = W_1 + \widehat{W}_1$ with $\widehat{W}_1 = 0$ on $|\mathbf{y}| = \ell_j$,

$$(4.19) \qquad W_1 \to \chi_j^{(1)} = -4\pi D \sum_{k=1}^{N} \Phi(\beta\ell_k)G_{k0}\ell_k\mathcal{G}_{jk} \text{ as } |\mathbf{y}| \to \infty$$

and

$$(4.20) \qquad \widehat{W}_1 \to \mathbf{b}_j \cdot \mathbf{y} \text{ as } |\mathbf{y}| \to \infty, \ \mathbf{b}_j = \nabla_{\mathbf{x}}G(\mathbf{x}_j, s|\mathbf{x}_0).$$

The general solutions for $W_1$ and $V_1$ are

$$(4.21) \qquad W_1 = \chi_j^{(1)} + A_1\frac{\ell_j}{|\mathbf{y}|}, \quad V_1 = B_1 I_{1/2}(\beta|\mathbf{y}|)/\sqrt{\beta|\mathbf{y}|}.$$

In terms of spherical polar coordinates $\rho = |\mathbf{y}|$, $\mathbf{b}_j = (0, 0, b_j)$, and $\mathbf{y} \cdot \mathbf{b}_j = b_j\rho\cos\theta$, $0 \leq \theta \leq \pi$, we have

$$(4.22) \qquad \frac{\partial^2\widehat{W}_1}{\partial\rho^2} + \frac{2}{\rho}\frac{\partial\widehat{W}_1}{\partial\rho} + \frac{1}{\rho^2\sin\theta}\frac{\partial}{\partial\theta}\left(\sin\theta\frac{\partial\widehat{W}_1}{\partial\theta}\right) = 0, \ \rho > 1,$$

$$(4.23) \qquad \widehat{W}_1 \sim b_j\rho\cos\theta \text{ as } \rho \to \infty; \quad \widehat{W}_1 = 0 \text{ on } \rho = \ell_j.$$

The general solution of Laplace's equation in spherical polar coordinates is given by

$$(4.24) \qquad B(\rho, \theta, \phi) = \sum_{l \geq 0}\sum_{m=-l}^{l}\left(a_{lm}\rho^l + \frac{b_{lm}}{\rho^{l+1}}\right)P_l^m(\cos\theta)e^{im\phi},$$

where $P_l^m(\cos\theta)$ is an associated Legendre polynomial. Imposing the Dirichlet boundary condition and the far-field condition implies that

$$(4.25) \qquad \widehat{W}_1(\mathbf{y}) = b_j\ell_j\cos\theta\left(\frac{|\mathbf{y}|}{\ell_j} - \frac{\ell_j^2}{|\mathbf{y}|^2}\right).$$

This will contribute to the far-field behavior of the $O(\epsilon^3)$ term in the outer solution. However, it does not contribute to the flux into a target. Also note that

$$(4.26) \qquad \nabla\widehat{W}_1(\mathbf{y}) \cdot \mathbf{n} = 3b_j\cos\theta \quad \text{on } |\mathbf{y}| = \ell_j.$$

We can now determine the unknown coefficients $A_1, B_1$ using the matching conditions

$$(4.27) \qquad W_1(\mathbf{y}) = V_1(\mathbf{y}), \quad \nabla W_1(\mathbf{y}) \cdot \mathbf{n} + \nabla \widehat{W}_1(\mathbf{y}) \cdot \mathbf{n}_j = \nabla V_1(\mathbf{y}) \cdot \mathbf{n}_j, \quad |\mathbf{y}| = \ell_j.$$

The matching conditions then imply that

$$(4.28a) \qquad \chi_j^{(1)} + A_1 = \frac{B_1}{\sqrt{\beta \ell_j}} I_{1/2}(\beta \ell_j),$$

$$(4.28b) \qquad -\frac{A_1}{\ell_j} + 3b_j \cos \theta = \frac{B_1}{\sqrt{\beta \ell_j}} \left[ \beta I'_{1/2}(\beta \ell_j) - \frac{1}{2\ell_j} I_{1/2}(\beta \ell_j) \right].$$

Hence,

$$(4.29) \qquad W_1 = \chi_j^{(1)} \left[ 1 - \Phi(\beta \ell_j) \frac{\ell_j}{|\mathbf{y}|} \right] + 3b_j \cos \theta [1 - \Phi(\beta \ell_j)] \frac{\ell_j^2}{|\mathbf{y}|}.$$

The analysis of $U_n$ for $n \geq 2$ is more complicated due to the fact that the equation for $V_n$, (4.5c), is now inhomogeneous. The case $n = 2$ is given in the appendix. One finds that $U_n$ has the general form

$$U_n(\mathbf{y}) = \chi_j^{(n)} - (\Phi(\beta \ell_j) \chi_j^{(n)} - w_j^{(n)}) \frac{\ell_j}{|\mathbf{y}|} + \widehat{w}_j^{(n)}(|\mathbf{y}|)$$

$$(4.30) \qquad\qquad + \text{ higher-order spherical harmonics},$$

where the coefficients $\chi_j^{(n)}$ satisfy the iterative equation

$$(4.31) \qquad \chi_j^{(n+1)} = -4\pi D \sum_{k=1}^{N} \Phi(\beta \ell_k) \chi_k^{(n)} \ell_k \mathcal{G}_{jk}, \quad n \geq 1.$$

Note that $w_j^{(0)} = \widehat{w}_j^{(0)} = 0$, whereas (4.25) and (4.29) yield the expressions $w_j^{(1)} = b_j \ell_j \cos(\theta)(1 - \Phi(\beta \ell_j))$ and $\widehat{w}_j^{(1)} = b_j \ell_j \cos(\theta) \left( |\mathbf{y}|/\ell_j - \ell_j^2/|\mathbf{y}|^2 \right)$. The calculations of $w_j^{(n)}$ and $\widehat{w}_j^{(n)}(\mathbf{y})$ are carried out in the appendix.

**4.3. The flux.** The $\epsilon$ expansion of the inner solution generates a corresponding expansion of the flux into the $j$th target. In particular, Laplace transforming (2.29) and rescaling by the factor $\kappa_1/(\kappa_1 + \epsilon^2 s)$ shows that

$$(4.32) \qquad \widetilde{J}_j(\mathbf{x}_0, s) = D\epsilon^2 \int_{|\mathbf{y}| = \ell_j} \nabla_{\mathbf{x}} U \cdot \mathbf{n}_j \, d\mathbf{y} \sim D\epsilon \int_{|\mathbf{y}| = \ell_j} [\nabla_{\mathbf{y}} U_0 + \epsilon \nabla_{\mathbf{y}} U_1 + \dots] \cdot$$
$$\mathbf{n}_j \, dS_{\mathbf{y}}.$$

Introducing spherical polar coordinates $(\rho, \theta, \phi)$ relative to the center of $\mathcal{U}_j$, we can rewrite the asymptotic expansion of the flux as

$$(4.33) \qquad \widetilde{J}_j(\mathbf{x}_0, s) \sim \epsilon \widetilde{J}_j^{(0)}(\mathbf{x}_0, s) + \epsilon^2 \widetilde{J}_j^{(1)}(\mathbf{x}_0, s) + \epsilon^3 \widetilde{J}_j^{(2)}(\mathbf{x}_0, s) + \dots$$

with

$$\widetilde{J}_j^{(n)} = D\ell_j^2 \int_0^{2\pi} \int_0^{\pi} \left. \frac{\partial}{\partial \rho} \right|_{\rho = \ell_j} \left[ -\frac{\ell_j [\Phi(\beta \ell_j) \chi_j^{(n)} - w_j^{(n)}]}{\rho} + \widehat{w}_j^{(n)}(\rho) \right] \sin \theta \, d\theta \, d\phi$$

$$(4.34) \qquad = 4\pi D \ell_j [\Phi(\beta \ell_j) \chi_j^{(n)} - w_j^{(n)}] + 4\pi D \ell_j^2 \left. \frac{d\widehat{w}_j^{(n)}}{d\rho} \right|_{\rho = \ell_j}.$$

In particular, the flux through the $j$th target is

$$\widetilde{J}_j(\mathbf{x}_0, s) \sim 4\pi\epsilon D\ell_j \Phi(\beta\ell_j) \left( G(\mathbf{x}_j, s|\mathbf{x}_0) - 4\pi\epsilon D \sum_{k=1}^{N} \Phi(\beta\ell_k) G(\mathbf{x}_k, s|\mathbf{x}_0)\ell_k \mathcal{G}_{jk}(s) \right)$$

(4.35)        $+ O(\epsilon^3).$

This expansion will be valid provided that $s \ll 1/\epsilon$. Several remarks are in order.

- (i) The series expansion (4.35) to $O(\epsilon^2)$ has a relatively straightforward dependence on the rescaled absorption rate $\kappa_1$. That is, each Green's function product of order $n$ is scaled by a factor of $\Phi(\beta\ell_j)^n$, where $\Phi(\beta\ell_j)$ is defined in (4.14) with $\beta = \sqrt{\kappa_1/D}$. However, there are additional terms at higher orders in $\epsilon$ that display a more complicated dependence on $\kappa_1$ due to the coefficients $w_j^{(n)}$ and $\widehat{w}_j^{(n)}$.
- (ii) Since $\Phi(\beta\ell_j) \to 1$ in the limit $\kappa_1 \to \infty$, we recover our previous result for totally absorbing targets [9]. On the other hand, $\Phi(\beta\ell_j) \to 0$ as $\kappa_1 \to 0$, which means that the net flux into each target vanishes in the absence of any absorption.
- (iii) Our previous analysis of the 3D narrow capture problem with totally absorbing targets established that the limit $s \to 0$ in (4.35) is nontrivial due to the small-$s$ singularity of the modified Helmholtz Green's function [9]:

$$G(\mathbf{x}, s|\mathbf{x}') = \frac{1}{s|\mathcal{U}|} + \overline{G}(\mathbf{x}, \mathbf{x}') + sF(\mathbf{x}, \mathbf{x}') + O(s^2),$$

(4.36)

where $\overline{G}(\mathbf{x}, \mathbf{x}')$ is the Neumann Green's function for the diffusion equation:

(4.37a)        $D\nabla^2 \overline{G}(\mathbf{x}; \mathbf{x}') = \frac{1}{|\mathcal{U}|} - \delta(\mathbf{x} - \mathbf{x}'), \ \mathbf{x} \in \mathcal{U}; \ \nabla\overline{G} \cdot \mathbf{n} = 0, \ \mathbf{x} \in \partial\mathcal{U},$

(4.37b)        $\overline{G}(\mathbf{x}, \mathbf{x}') = \frac{1}{4\pi D|\mathbf{x} - \mathbf{x}'|} + \overline{R}(\mathbf{x}, \mathbf{x}'), \quad \int_{\mathcal{U}} \overline{G}(\mathbf{x}, \mathbf{x}')d\mathbf{x} = 0,$

and $\overline{R}(\mathbf{x}, \mathbf{x}')$ is regular part of $\overline{G}(\mathbf{x}, \mathbf{x}')$. Substitution of (4.36) into (4.35) leads to terms involving factors of $\epsilon/r$, which become arbitrarily large as $r \to 0$, thus leading to a breakdown of the $\epsilon$ expansion. Following along analogous lines to [9], it is possible to perform a partial resummation of the asymptotic expansion that renders the resulting series nonsingular in the limit $r \to 0$. The basic idea is to introduce a new dimensionless parameter

(4.38)        $$\Lambda = \frac{4\pi\epsilon D\overline{\ell}}{r|\mathcal{U}|}.$$

This converts a subset of $O(\epsilon^n)$ terms in the expansion of $\widetilde{J}_j$ to $O(\epsilon^r \Lambda^{n-r})$ terms, $0 \le r \le n$. At each order of $\epsilon$, we obtain an infinite power series in $\Lambda$ that can be summed to remove all singularities in the limit $r \to 0$. Following similar steps to [9], we find that

$$\widetilde{J}_j(\mathbf{x}_0, r) \sim 4\pi\epsilon D\ell_j \Phi(\beta\ell_j)\overline{G}_{j0} + \frac{\ell_j}{\overline{\ell}} \frac{\Lambda}{1 + \Lambda} \left[ 1 - 4\pi\epsilon D\Phi(\beta\ell_j) \sum_k \Phi(\beta\ell_k)\ell_k(\overline{G}_{k0} + \overline{\mathcal{G}}_{jk}) \right]$$

(4.39)        $+ \frac{4\pi\epsilon\ell_j D\Phi(\beta\ell_j)}{\overline{\ell}^2} \frac{\Lambda^2}{(1 + \Lambda)^2} \sum_{i,k=1}^{N} \Phi(\beta\ell_i)\Phi(\beta\ell_k)\ell_i \overline{\mathcal{G}}_{ik}\ell_k + O(\epsilon^2, r).$

We can now safely take the limit $r \to 0$ for $\epsilon > 0$ with $\Lambda \to \infty$.

(iv) For simplicity, we have considered spherically shaped targets. However, as originally shown by Ward and Keller [37], it is possible to generalize the asymptotic analysis of narrow capture problems to more general target shapes such as ellipsoids by applying classical results from electrostatics. In the case of totally absorbing targets one simply replaces the target length $\ell_j$ in the far-field behavior of the inner solution by the capacitance $C_j$ of an equivalent charged conductor with the shape $\mathcal{U}_j$. In addition, using the divergence theorem, it can then be shown that the flux into a target is completely determined by the far-field behavior. However, the analysis is more complicated when considering partially absorbing targets, since it is necessary to match the solution $U(\mathbf{y})$ exterior to a target with the solution $V(\mathbf{y})$ inside the target. The latter would require solving the modified Helmholtz equation in a nonspheroidal shape $\mathcal{U}_j$.

**4.4. Pair of targets in a sphere.** We now combine our $O(\epsilon^2)$ asymptotic expansion of the flux given by (4.35) with the expressions (2.26) and (2.27) for the splitting probability $\pi_r(\mathbf{x}_0)$ and unconditional MFPT $T_r(\mathbf{x}_0)$, respectively, by identifying the Laplace variable $s$ with the resetting rate $r$. For the sake of illustration, suppose that the search domain is a sphere of radius $\rho_0$. Consider two targets of equal size $\ell_j = 1$ located along a diagonal at a distance $\rho_j$ from the center, $j = 1, 2$; see Figure 4.1(a). The Neumann Green's function of the modified Helmholtz equation and of the diffusion equation can be calculated explicitly for a spherical domain as detailed in [25, 9]. In Figure 4.1(b) we plot the splitting probabilities $\pi_{r,k}$, $k = 1, 2$, as a function of the resetting rate $r$ for $\epsilon \ll r \ll 1/\epsilon$. (The lower bound is imposed due to the singular nature of the Green's functions in the limit $r \to 0$; see remark (iii).) We also take $\rho_1 + \rho_2 = 1$. Clearly if $\rho_1 = \rho_2$, then each particle is equally likely to be absorbed by either target and $\pi_{r,1} = \pi_{r,2} = 1/2$. However, if $\rho_1 < \rho_2$, then the particle is more likely to be absorbed by the target closer to the origin, that is, $\pi_{r,1} > \pi_{r,2}$. We
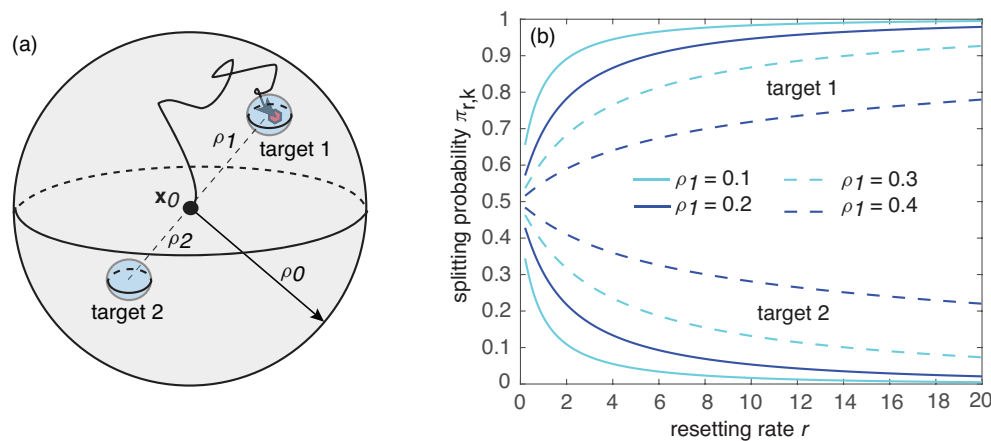


FIG. 4.1. (a) 3D spherical search domain of radius $r = \rho_0$ containing two diagonally opposed targets at distances $r_j$ from the center. The initial position of the searcher is taken to be at the center of the sphere, $\mathbf{x}_0 = 0$. (b) Plot of splitting probabilities $\pi_{r,k}(\mathbf{x}_0)$, $k = 1, 2$, for $\mathbf{x}_0 = 0$. The splitting probabilities are determined by equations (2.26) and (4.35). The distance of the targets are varied such that $\rho_1 + \rho_2 = 1$. Other parameter values are $D = 1$, $\ell_j = 1$, $\rho_0 = 1$, and $\epsilon = 0.01$. The plots are insensitive to the value of $\kappa_1$ for $\epsilon \ll 1$.
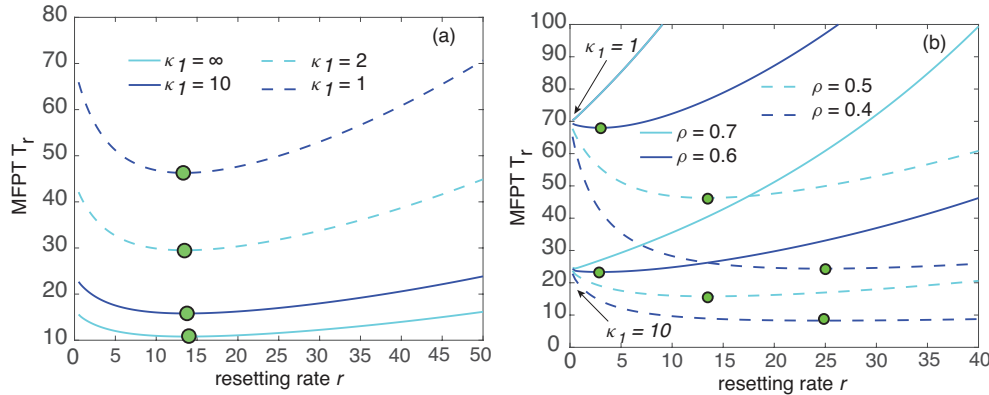
FIG. 4.2. *Plot of unconditional MFPT $T_r(\mathbf{x}_0)$ as a function of $r$ for the pair of targets shown in Figure 4.1 with $\mathbf{x}_0 = 0$. The MFPT is determined by (2.27) and (4.35). (a) The distance of the targets are fixed at $\rho_1 = \rho_2 = 0.5$ and the absorption rate $\kappa_1$ is varied. The filled circles indicate the optimal resetting rate for a given $\kappa_1$. (b) Fixed $\kappa_1$ and different target distances $\rho = \rho_{1,2}$. The filled circles indicate the optimal resetting rate for a given $\rho$ and $\kappa_1$. Other parameter values are $D = 1$, $\ell_j = 1$, $\rho_0 = 1$, and $\epsilon = 0.01$.*

see from Figure 4.1(b) that this difference increases with $r$. Analogous results were obtained in our previous study [9]. The additional observation here is that the splitting probabilities are only weakly dependent on the absorption rate $\kappa_1$ and the target size $\epsilon$. Therefore, in order to investigate the effects of partially absorbing targets, we consider the MFPT $T_r(\mathbf{x}_0)$. Plots of $T_r(\mathbf{x}_0)$ versus $r$ are shown in Figure 4.2(a). The results are similar to the 2D case. For target distances smaller than a critical value $\rho_c$, the MFPT is a unimodal function of $r$ with a minimum at an optimal resetting rate $r_{\mathrm{opt}}$. In addition, $r_{\mathrm{opt}}$ is only weakly dependent on the absorption rate $\kappa_1$ compared to other parameter values. For example, in Figure 4.2(b) we plot $T_r(\mathbf{x}_0)$ against $r$ for different distances $\rho = \rho_{1,2}$, which clearly show a large variation of $r_{\mathrm{opt}}$.

**5. Stochastic simulations.** In order to test the validity of the asymptotic expansions, a stochastic algorithm was implemented and the analytical results were compared to a series of Monte Carlo simulations. The algorithm uses a modified walk-on-spheres method that accommodates partial absorption and stochastic resetting to improve computational efficiency when $N\epsilon^d \ll 1$. Let $\mathbf{x}(t) \in \mathbb{R}^d$ be the position of a diffusing particle at time $t$ with $d = 2, 3$ and $\mathbf{x}_0 = \mathbf{x}(0)$. Assume that the particle is diffusing in a bounded spherical domain $\Omega \subset \mathbb{R}^d$ with radius $R$ that contains spherical partially absorbing targets $\mathcal{U}_1, \ldots, \mathcal{U}_N \subset \Omega$ with radii $\epsilon \ll 1$ positioned at $\mathbf{x}_1, \ldots, \mathbf{x}_N$, respectively. We also place a boundary layer of width $\delta$ around the outside of each target and the region inside of $\Omega$ adjacent to $\partial\Omega$. The algorithm can be described with the following steps:

1. Place the particle at $\mathbf{x}_0$ and let $t_r = t + \Delta t_r$ be the next time at which the particle resets where $\Delta t_r$ is a random variable with PDF $\psi(t) = re^{-rt}$, $t \geq 0$, where $r$ is the resetting rate.
2. Compute $\rho_b = R - \|\mathbf{x}(t)\|$ and $\rho_t = \min_{n=1,\ldots,N} \|\mathbf{x}(t) - \mathbf{x}_n\| - \epsilon$ and put $\rho = \min\{\rho_b, \rho_t\}$. If $\rho > \delta$, then proceed to step 3. If $0 \leq \rho \leq \delta$, proceed to step 4. If $\rho < 0$, proceed to step 5.
3. Sample a random time, $\Delta\hat{t}$, that has CDF $F(t) = 1 - S(t, 0)$ where $S(t, y)$ is the survival probability for a diffusing particle to escape the inside of a

$d$-dimensional sphere with radius 1 given that the particle started at a distance $y$ from the center of the sphere. One can obtain $S(t, y)$ by numerically solving the PDE

$$(5.1) \qquad D^{-1}\frac{\partial S}{\partial t} = \frac{\partial^2 S}{\partial y^2} + \frac{d-1}{y}\frac{\partial S}{\partial y},$$

$$(5.2) \qquad S(0, y) = 1, \quad y < 1,$$

$$(5.3) \qquad S(t, 1) = \left.\frac{\partial S}{\partial y}\right|_{y=0} = 0.$$

We can now sample $\Delta\widehat{t}$ by noting that $\Delta\widehat{t} = F^{-1}(U)$ where $U \in [0, 1]$ is a uniform random variable and applying the inverse CDF method. The time it takes a particle to escape a spherical region with radius $r$ given the particle started at the center of the sphere is $\Delta t_s = r^2 \Delta\widehat{t}$. If $t + \Delta t_s \geq t_r$, then reset the diffusion process by letting $t \to t + t_r$ and returning to step 1. Otherwise, let $t \to t + \Delta t_s$ and $\Delta\mathbf{x}$ be a random vector such that the tail of the vector is at $\mathbf{x}(t)$ and the tip is at a point sampled uniformly from the surface of a $d$-dimensional sphere centered at $\mathbf{x}(t)$ with radius $r$. Let $\mathbf{x}(t) \to \mathbf{x}(t) + \Delta\mathbf{x}$ and return to step 2.

4. If $t \geq t_r$, reset the diffusion process using the same method as that used in step 3. Otherwise, perform an Euler–Maruyama iteration by generating a $d$-dimensional vector $\Gamma$ from a multivariate standard normal distribution, letting $t \to t + \Delta t_{\text{EM}}$, and letting $\mathbf{x}(t) \to \mathbf{x}(t) + \sqrt{2D\Delta t_{\text{EM}}}\Gamma$, where $\Delta t_{\text{EM}}$ is a fixed parameter describing the step size. Now return to step 2.

5. If $\mathbf{x}(t - \Delta t_{\text{EM}}) \notin \cup_{i=1}^n \mathcal{U}_i$, then generate a number $\Delta t_a$ by randomly sampling a set of times according to the PDF $\phi(t) = \kappa e^{-\kappa t}$, $t \geq 0$, where $\kappa = \kappa_1/\epsilon^2$ is the absorption rate, and let $t_a = t + \Delta t_a$ be the next time at which the particle is absorbed. Now, move to step 4. If $\mathbf{x}(t - \Delta t_{\text{EM}}) \in \cup_{i=1}^n \mathcal{U}_i$, then check if $t \geq t_a$. If this inequality holds, the simulation ends and $t_a$ is recorded as the FPT. If $t < t_a$, proceed to step 4.

It is important to note that each time the particle leaves and re-enters a target, a new absorption time, $t_a$, is generated. Therefore, a particle is only absorbed if it enters a target and spends $\Delta t_a$ units of time in the target without leaving. Similarly, a new time, $\Delta t_r$, is generated each time the particle resets. Figures 5.1 and 5.2 show good agreement between the MFPTs derived from the simulations and those obtained from (3.18) and (4.35). Note that the error rate increases for $\epsilon$ near 0.01 for the 3D simulations. This is due to the fact that $2\epsilon^3$ is very small. Therefore, accuracy can be improved by decreasing $\Delta t_{\text{EM}}$ and increasing the total number of simulations that are averaged over.

**6. Discussion.** In this paper we analyzed the narrow capture problem in 2D and 3D under the joint effects of stochastic resetting and partially absorbing targets. By matching inner and outer solutions of the diffusion equation in Laplace space, we derived an asymptotic expansion of the flux $\widetilde{J}_k$ into each target in powers of $\nu = -1/\ln\epsilon$ in 2D and powers of $\epsilon$ in 3D, where $\epsilon$ is the non-dimensionalized target size. (In the former case, all logarithmic terms were summed over nonperturbatively.) This then determined the MFPT to absorption according to the formula $T_r(\mathbf{x}_0) = (1 - \sum_{k=1}^N \widetilde{J}_k(\mathbf{x}_0, r))/(r\sum_{j=1}^N \widetilde{J}_j(\mathbf{x}_0, r))$ for a resetting rate $r$. We illustrated the theory by considering spherically symmetric targets. We determined the MFPT to absorption as a function of $r$, $\kappa$, and the target distances from the resetting point,
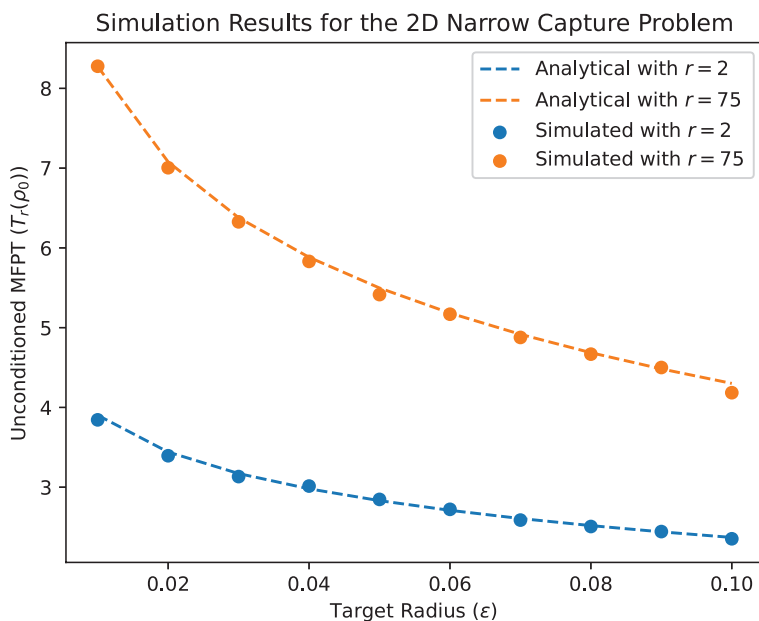
Fig. 5.1. *Comparison of the analytical MFPT plots with numerical results generated by simulating the 2D narrow capture problem with two partially absorbing targets using algorithm* [5] *and averaging over* $10^4$ *simulations. Other parameter values were* $R = 5$, $\mathbf{x}_1 = [1,0]^T$, $\mathbf{x}_2 = [-1.5, 0]$, $\kappa_1 = 1$, $\delta = 0.1$, $\Delta t_{EM} = 10^{-6}$, *and* $D = 1$.
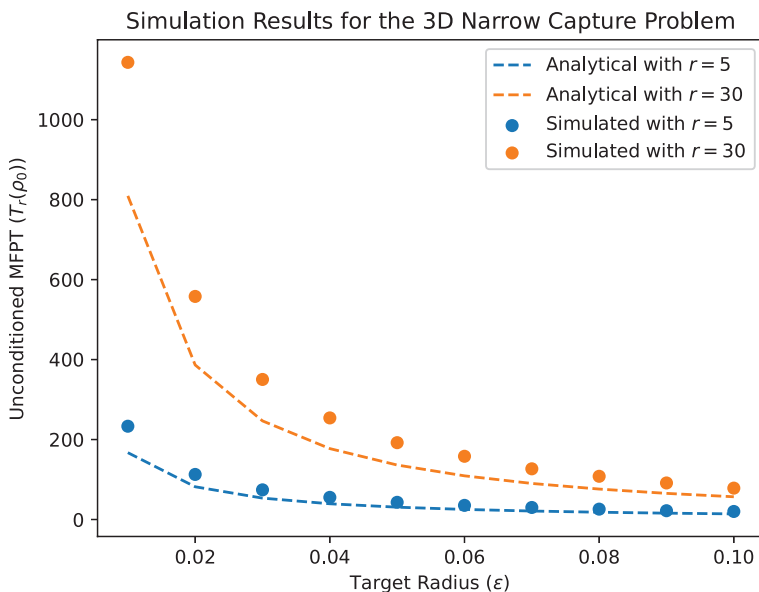


Fig. 5.2. *Comparison of the analytical MFPT plots with numerical results generated by simulating the* 3D *narrow capture problem with two partially absorbing targets using algorithm* [5] *and averaging over* $10^4$ *simulations. Other parameter values include* $R = 5$, $\mathbf{x}_1 = [1,0,0]^T$, $\mathbf{x}_2 = [-1.5, 0, 0]$, $\kappa_1 = 1$, $\delta = 0.1$, $\Delta t_{EM} = 10^{-8}$, *and* $D = 1$.

and we explored the behavior of the optimal resetting rate as a function of model parameters.

The analysis of partially absorbing targets developed in this paper has a wide variety of possible extensions. First, as indicated at the end of section 4.3 , one could consider more general target shapes by numerically solving the modified Helmholtz equation within each target and matching with the inner solution outside the target. Second, one could incorporate a more general chemical kinetic scheme within each target, rather than assuming direct absorption. For example, on entering a target, the particle could reversibly bind to the chemical substrate and undergo a sequence of reversible reactions before being absorbed [36]. Alternatively, the reaction scheme could be non-Markovian, analogous to a study of anomalous diffusion within spiny dendrites [21]. In this specific application particles diffuse along a one-dimensional dendritic cable that is studded with partially absorbing spines. The exchange of a particle between a spine and the parent dendrite is described by a non-Markovian stochastic process and leads to subdiffusive transport. It would also be interesting to explore the general probabilistic formulation of partially reactive surfaces developed in [23, 25, 10]. Finally, rather than assuming that the boundary of a target is fully permeable to a diffusing particle, one could consider a semipermeable membrane. The boundary conditions (2.1)c would be replaced by the following equations on $\mathbf{x} \in \partial \mathcal{U}_i$:

$$(6.1) \quad D\nabla q(\mathbf{x}, t|\mathbf{x}_0) \cdot \mathbf{n}_i = -\sigma[q(\mathbf{x}, t|\mathbf{x}_0) - p_i(\mathbf{x}, t|\mathbf{x}_0)], \quad D\nabla q(\mathbf{x}, t|\mathbf{x}_0) = D\nabla p_i(\mathbf{x}, t|\mathbf{x}_0),$$

where $\sigma$ is a membrane permeability coefficient. A special case of the above is to treat each target as a spatially homogeneous compartment, as exemplified by a model of bacterial quorum sensing [22].

**Appendix A. Calculation of $U_2$.** In order to calculate the inner contribution $U_2$, we have to match the far-field behavior of $U_2$ with the $O(\epsilon^2)$ term in the expansion of $\widetilde{q}_0$ (see (4.9)), the $O(\epsilon)$ terms in the expansion of $\widetilde{q}_1$, and the near-field behavior of $\widetilde{q}_2$ around $\mathcal{U}_j$. The latter satisfies (4.3) supplemented by the singularity condition

$$\widetilde{q}_2(\mathbf{x}, s) \sim -\Phi(\beta\ell_j)\frac{\chi_j^{(1)}\ell_j}{|\mathbf{x} - \mathbf{x}_j|} \quad \text{as } \mathbf{x} \to \mathbf{x}_j.$$

Following the same steps as in the derivation of $\widetilde{q}_1(\mathbf{x}, s)$ yields

$$(A.1) \qquad \widetilde{q}_2(\mathbf{x}, s) = -4\pi D \sum_{k=1}^{N} \Phi(\beta\ell_k)\chi_k^{(1)}\ell_k G(\mathbf{x}, s|\mathbf{x}_k).$$

Hence,

$$(A.2) \qquad U_2(\mathbf{y}, s) \to \frac{1}{2}\mathbf{H}_j \cdot \mathbf{y} \otimes \mathbf{y} + \nabla\tilde{q}_1|_{\mathbf{x}=\mathbf{x}_j} \cdot \mathbf{y} - 4\pi D\Phi(\beta\ell_j)\sum_{k=1}^{N}\chi_k^{(1)}\ell_k\mathcal{G}_{jk}$$

as $|\mathbf{y}| \to \infty$. In addition, setting $n = 2$ in (4.5), we have

$$(A.3) \qquad D\Delta_{\mathbf{y}}U_2 = sU_0, \ |\mathbf{y}| > \ell_j, \quad D\Delta_{\mathbf{y}}V_2 - \kappa_1 V_2 = sV_0, \ |\mathbf{y}| < \ell_j,$$

$$(A.4) \qquad U_2 = V_2, \quad \nabla U_2 \cdot \mathbf{n}_j = \nabla V_2 \cdot \mathbf{n}_j \text{ on } |\mathbf{y}| = \ell_j.$$

Again we decompose the inner term as $U_2 = W_2 + \widehat{W}_2$ with

$$(A.5) \quad \Delta_{\mathbf{y}}W_2 = 0, |\mathbf{y}| > \ell_j; \ W_2 \to \chi_j^{(2)} \equiv -4\pi D\Phi(\beta\ell_j)\sum_{k=1}^{N}\chi_k^{(1)}\ell_k\mathcal{G}_{jk} \text{ as } |\mathbf{y}| \to \infty,$$

and

(A.6)
$$D\Delta_{\mathbf{y}}\widehat{W}_2 = sU_0, \ |\mathbf{y}| > \ell_j; \ \widehat{W}_2 = 0, \ \text{on} \ |\mathbf{y}| = \ell_j,$$
$$\widehat{W}_2 \to \frac{1}{2}\mathbf{H}_j \cdot \mathbf{y} \otimes \mathbf{y} + \nabla\tilde{q}_1|_{\mathbf{x}=\mathbf{x}_j} \cdot \mathbf{y} \ \text{as} \ |\mathbf{y}| \to \infty.$$

The general solutions for $W_2$ and $V_2$ are

(A.7)
$$W_2 = \chi_j^{(2)} + A_2\frac{\ell_j}{|\mathbf{y}|}, \quad V_2 = B_2\frac{I_{1/2}(\beta|\mathbf{y}|)}{\sqrt{\beta|\mathbf{y}|}} + s\widehat{V}_2(\mathbf{y}, s; \kappa_1),$$

where $\widehat{V}_2$ is the particular solution with boundary condition $\widehat{V}_2(\mathbf{y}, s; \kappa_1) = 0$ on $|\mathbf{y}| = \ell_j$ (convolution of the Green's function in the sphere with $V_0$.) The explicit expression for $\widehat{V}_2(\mathbf{y}, s; \kappa_1)$ will not be needed in this paper.

The calculation of $\widehat{W}_2$ proceeds along analogous lines to [9], so we simply summarize the results here. First note that the particular solution of the equation $D\Delta_{\mathbf{y}}\widehat{W}_2 = sU_0$ has the explicit form

(A.8)
$$\widehat{W}_2\Big|_{\text{particular}} = \frac{s}{D}\left(\frac{\rho^2}{6} - \frac{\rho\ell_j\Phi(\beta\ell_j)}{2}\right)G(\mathbf{x}_j, s|\mathbf{x}_0).$$

It turns out that this matches the $l = 0$ component of the far-field condition, since

$$\frac{1}{2}\mathbf{H}_j \cdot \mathbf{y} \otimes \mathbf{y} + \nabla\tilde{q}_1 \cdot \mathbf{y} = \frac{\rho^2}{6}(H_{xx} + H_{yy} + H_{zz}) + \text{higher-order spherical harmonics},$$

and

$$\frac{\rho^2}{6}(H_{xx} + H_{yy} + H_{zz}) = \frac{\rho^2}{6}\Delta G(\mathbf{x}_i, s|\mathbf{x}_0) = \frac{\rho^2 s}{6D}G(\mathbf{x}_i, s|\mathbf{x}_0).$$

Hence, the only contribution to the flux integral from the component $\widehat{W}_2$ arises from the above particular solution. Finally, the unknown constants $A_2, B_2$ are determined by the boundary conditions at $|\mathbf{y}| = \ell_j$:

(A.9)
$$\chi_j^{(2)} + A_2 = B_2 I_{1/2}(\beta\ell_j)/\sqrt{\beta\ell_j},$$
$$-\frac{A_2}{\ell_j} + \frac{s\ell_j}{6D}\left(2 - 3\Phi(\beta\ell_j)\right)G(\mathbf{x}_j, s|\mathbf{x}_0) + \Theta_{2,j} = \frac{B_2}{\sqrt{\beta\ell_j}}\left[\beta I'_{1/2}(\beta\ell_j) - \frac{1}{2\ell_j}I_{1/2}(\beta\ell_j)\right]$$
$$+ \widehat{V}_2{}'(\ell_j, s; \kappa_1).$$

We have defined

(A.10)
$$\Theta_{2,j} = \mathbf{n}_j \cdot \nabla\left(\widehat{W}_2 - \widehat{W}_2\Big|_{\text{particular}}\right)_{|\mathbf{y}|=\ell_j},$$

which collects together all terms involving higher-order spherical harmonics.

## REFERENCES

[1] O. BENICHOU, C. CHEVALIER, J. KLAFTER, B. MEYER, AND R. VOITURIEZ, *Geometry-controlled kinetics*, Nat. Chem., 2 (2010), pp. 472–477.

[2] O. BENICHOU, C. LOVERDO, M. MOREAU, AND R. VOITURIEZ, *Intermittent search strategies*, Rev. Mod. Phys., 83 (2011), pp. 81–129.

[3] A. S. BODROVA AND I. M. SOKOLOV, *Resetting processes with noninstantaneous return*, Phys. Rev. E, 101 (2020), 052130.

[4] P. C. BRESSLOFF, B. A. EARNSHAW, AND M. J. WARD, *Diffusion of protein receptors on a cylindrical dendritic membrane with partially absorbing targets*, SIAM J. Appl. Math., 68 (2008), pp. 1223–1246, https://doi.org/10.1137/070698373.

[5] P. C. BRESSLOFF, *Modeling active cellular transport as a directed search process with stochastic resetting and delays*, J. Phys. A, 53 (2020), 355001.

[6] P. C. BRESSLOFF, *Search processes with stochastic resetting and multiple targets*, Phys. Rev. E, 102 (2020), 022115.

[7] P. C. BRESSLOFF, *Queuing model of axonal transport*, Brain Multiphys., 2 (2021), 100042.

[8] P. C. BRESSLOFF, *Asymptotic analysis of extended two-dimensional narrow capture problems*, Proc R. Soc. A, 477 (2021), 20200771.

[9] P. C. BRESSLOFF, *Asymptotic analysis of target fluxes in the three-dimensional narrow capture problem*, Multiscale Model. Simul., 19 (2021), pp. 612–632, https://doi.org/10.1137/20M1380326.

[10] P. C. BRESSLOFF, *Diffusion-mediated absorption by partially reactive targets: Brownian functionals and generalized propagators*, J. Phys. A, 55 (2022), 205001.

[11] A. CHECHKIN AND I. M. SOKOLOV, *Random search with resetting: A unified renewal approach*, Phys. Rev. Lett., 121 (2018), 050601.

[12] C. CHEVALIER, O. BENICHOU, B. MEYER, AND R. VOITURIEZ, *First-passage quantities of Brownian motion in a bounded domain with multiple targets: A unified approach*, J. Phys. A, 44 (2011), 025002.

[13] A. F. CHEVIAKOV AND M. J. WARD, *Optimizing the principal eigenvalue of the laplacian in a sphere with interior traps*, Math. Comp. Model., 53 (2011), 042118.

[14] D. COOMBS, R. STRAUBE, AND M. J. WARD, *Diffusion on a sphere with localized traps: Mean first passage time, eigenvalue asymptotics, and Fekete points*, SIAM J. Appl. Math., 70 (2009), pp. 302–332, https://doi.org/10.1137/080733280.

[15] M. I. DELGADO, M. WARD, AND D. COOMBS, *Conditional mean first passage times to small traps in a 3-D domain with a sticky boundary: Applications to T cell searching behavior in lymph nodes*, Multiscale Model. Simul., 13 (2015), pp. 1224–1258, https://doi.org/10.1137/140978314.

[16] M. R. EVANS AND S. N. MAJUMDAR, *Diffusion with stochastic resetting*, Phys. Rev. Lett., 106 (2011), 160601.

[17] M. R. EVANS AND S. N. MAJUMDAR, *Diffusion with optimal resetting*, J. Phys. A Math. Theor., 44 (2011), 435001.

[18] M. R. EVANS AND S. N. MAJUMDAR, *Diffusion with resetting in arbitrary spatial dimension*, J. Phys. A Math. Theor., 47 (2014), 285001.

[19] M. R. EVANS AND S. N. MAJUMDAR, *Effects of refractory period on stochastic resetting*, J. Phys. A Math. Theor., 52 (2019), 01LT01.

[20] M. R. EVANS, S. N. MAJUMDAR, AND G. SCHEHR, *Stochastic resetting and applications*, J. Phys. A Math. Theor., 53 (2020), 193001.

[21] S. FEDOTOV AND V. MÉNDEZ, *Non-Markovian model for transport and reactions of particles in spiny dendrites*, Phys. Rev. Lett., 101 (2008), 218102.

[22] J. GOU AND M. J. WARD, *Asymptotic analysis of a 2-D Model of dynamically active compartments coupled by bulk diffusion*, J. Nonlinear Sci., 26 (2016), pp. 979–1029.

[23] D. S. GREBENKOV, *Imperfect diffusion-controlled reactions*, IN Chemical Kinetics: Beyond the Textbook, K. LINDENBERG, R. METZLER, AND G. OSHANIN, eds., World Scientific, Singapore, 2019, pp. 191–219.

[24] D. S. GREBENKOV, *Paradigm shift in diffusion-mediated surface phenomena*, Phys. Rev. Lett., 125 (2020), 078102.

[25] D. S. GREBENKOV, *Diffusion toward non-overlapping partially reactive spherical traps: Fresh insights onto classic problems*, J. Chem. Phys., 152 (2020), 244108.

[26] P. HANGGI, P. TALKNER, AND M. BORKOVEC, *Reaction-rate theory: Fifty years after Kramers*, Rev. Mod. Phys., 62 (1990), pp. 251–341.

[27] V. KURELLA, J. C. TZOU, D. COOMBS, AND M. J. WARD, *Asymptotic analysis of first passage time problems inspired by ecology*, Bull. Math. Biol., 77 (2015), pp. 83–125.

[28] A. E. LINDSAY, T. KOLOKOLNIKOV, AND J. C. TZOU, *Narrow escape problem with a mixed trap and the effect of orientation*, Phys. Rev. E, 91 (2015), 032111.

[29] A. E. LINDSAY, R. T. SPOONMORE, AND J. C. TZOU, *Hybrid asymptotic-numerical approach for estimating first-passage-time densities of the two-dimensional narrow capture problem*, Phys. Rev. E, 94 (2016), 042418.

[30] A. E. Lindsay, A. J. Bernoff, and M. J. Ward, *First passage statistics for the capture of a Brownian particle by a structured spherical target with multiple surface targets*, Multiscale Model. Simul., 15 (2017), pp. 74–109, https://doi.org/10.1137/16M1077659.

[31] C. Loverdo, O. Benichou, M. Moreau, and R. Voituriez, *Enhanced reaction kinetics in biological cells*, Nat. Phys., 4 (2008), pp. 134–137.

[32] D. Maso-Puigdellosas, A. Campos, and V. Mendez, *Transport properties of random walks under stochastic noninstantaneous resetting*, Phys. Rev. E, 100 (2019), 042104.

[33] A. Maso-Puigdellosas, D. Campos, and V. Mendez, *Stochastic movement subject to a reset-and-residence mechanism: Transport properties and first arrival statistics*, J. Stat. Mech. Theory Exp., 2019 (2019), 033201.

[34] A. Pal, L. Kusmierz, and S. Reuveni, *Home-range search provides advantage under high uncertainty*, Phys. Rev. Res., 2 (2020), 043174.

[35] S. A. Rice, *Diffusion-Limited Reactions*, Elsevier, Amsterdam, 1985.

[36] R. D. Schumm and P. C. Bressloff, *Search processes with stochastic resetting and partially absorbing targets*, J. Phys. A, 54 (2021), 404004.

[37] M. J. Ward and J. B. Keller, *Strong localized perturbations of eigenvalue problems*, SIAM J. Appl. Math., 53 (1993), pp. 770–798, https://doi.org/10.1137/0153038.